Methylation of TMEM176A, a Key ERK Signaling Regulator, is a Novel Synthetic Lethality Marker of ATM Inhibitor in Human Lung Cancer

Hongxia Li
Chinese PLA General Hospital
Weili Yang
Chinese PLA General Hospital
Tao He
Chinese PLA General Hospital
Fuyou Zhou
Anyang Cancer Hospital
James G Herman
University of Pittsburgh Cancer Institute: UPMC Hillman Cancer Center
Liming Hu
Beijing University of Technology
Mingzhou Guo (mzguo@hotmail.com)
Chinese PLA General Hospital https://orcid.org/0000-0002-9445-9984

Research

Keywords: TMEM176A, DNA Methylation, synthetic lethality, ERK pathway, AZD0156

Posted Date: November 11th, 2020

DOI: https://doi.org/10.21203/rs.3.rs-99585/v1

Version of Record: A version of this preprint was published at Epigenomics on September 24th, 2021. See the published version at https://doi.org/10.2217/epi-2021-0217.

Abstract

Background: Synthetic lethality is a new strategy of cancer therapy. Epigenetic based synthetic lethality may provide more opportunities for cancer prevention and treatment. TMEM176A is frequently methylated in esophageal, hepatic and colorectal cancer**.** The role of TMEM176A methylation in lung cancer and its therapeutic application remains unclear.

Methods: Nine lung cancer cell lines and 123 cases of cancer tissue samples were employed. Methylation specific PCR, MTT assay, flow cytometry, and xenograft mouse models were applied.

Results: The expression of TMEM176A was found to be regulated by promoter region methylation in lung cancer cells. TMEM176A was methylated in 53.66% (66/123) of primary lung cancer. Reduced expression of TMEM176A was associated with promoter region methylation in 40 cases of matched lung cancer and adjacent tissue samples (P<0.05). No association was found between TMEM176A methylation and age, gender, alcohol abuse, smoking, tumor size, lymph node metastasis, differentiation and TNM stage (all P >0.05). Restoration of TMEM176A expression induced cell apoptosis and G2/M phase arrest and inhibited colony formation, cell proliferation, migration and invasion in H1299 and H23 cells. TMEM176A suppressed H1299 cell xenograft growth in mice. Methylation of TMEM176A activated ERK1/2 signaling, and sensitized H1299 and H23 cells to AZD0156, an ATM inhibitor.

Conclusion: TMEM176A is frequently methylated in human lung cancer, and the expression of TMEM176A is regulated by promoter region methylation. TMEM176A suppresses lung cancer growth by inhibiting ERK1/2 signaling. Methylation of TMEM176A is a potential lung cancer diagnostic marker and a novel synthetic lethal therapeutic marker for AZD0156, an ATM inhibitor.

Background

Lung cancer is one of the most common cancers and the first leading cause of cancer related death worldwide (1). Tobacco consumption is considered as the most important risk factor for the development of lung cancer (2). While, it is currently well established that an important percentage of never smokers is diagnosed with lung cancer (3). Many other risk factors have been described, including radon, asbestos exposure, domestic fuel smoke and HPV infection (2, 3). The mechanism of lung cancer development remains unclear. Aberrant genetic and epigenetic changes are involved in tumorigenesis and progression (4, 5).

The identification of actionable oncogenic mutations has greatly improved the treatment of different cancers (6–8). In non-small cell lung cancers (NSCLCs), the discovery of activating mutations in the epidermal growth factor receptor (EGFR) gene have ushered in a new era of genomics-guided precision targeted therapy in lung cancer(9). Advances in the knowledge of pathway, newly developed drugs to block the activities of signaling pathways in recent years have allowed the physicians to tailor the treatment options (8, 10). Nevertheless, this unprecedented benefit from current standard therapies is still observed in only a minority of patients.

Aberrant epigenetic changes have been reported in various cancers, including lung cancer (4, 5, 11, 12). It is now a well-established concept that epigenetic alterations are driver events in the pathogenesis of human cancers. In contrast to ‘mut-driver genes’, a greater number of ‘epi-driver genes’ are abnormally expressed by aberrant epigenetic changes in human cancers(13). Cancer-related signaling pathways may be disrupted by a key component aberrant methylation. Currently, epigenetic therapies are successfully used in the clinic to treat hematological malignancies. However, little success has been achieved in treating solid tumors. Novel epigenome-based therapeutic strategies are developing, including “synthetic lethality”(10, 14, 15). The concept of synthetic lethality originates from studies in Drosophila model systems in which a combination of mutations in 2 or more separate genes leads to cell death (16). In 2005, 2 groups described the synthetic lethality interaction between PARP inhibition and BRCA1 and BRCA2 mutation, and developed a novel treatment strategy for BRCA-mutant tumors(17, 18). The synthetic lethality approach has been applied in various dysfunctional BRCA1 and BRCA2 cancers(19). ‘BRCAness’ means a homologous recombination repair (HR) defect phenotype beyond the narrow scope of BRCA1 or BRCA2 mutation. It is similar to gene mutations that epigenetic silencing of tumor suppressor genes may cause inactivation or ‘loss-of-function’ in these genes. Thus, epigenetics joins Knudson’s two hit theory. DNA damage repair (DDR) and cell cycle regulator genes were found frequently methylated in human cancers. It is reasonable to apply the aberrant epigenetic changes to synthetic lethal therapy in human cancers. However, epigenetic-based synthetic lethal has not been extensively studied. Thus, it is important to identify the predictive biomarker of response and /or resistance to DDR inhibitors.

Human transmembrane protein 176A (TMEM176A) was first identified by screening tumor related antigens in hepatocellular carcinoma (HCC) (20, 21). Most of studies were mainly focused on its function in development and the immune system (22–24). Our previous study found that the expression of TMEM176A was reduced in human colorectal cancer tissue compared to normal colorectal mucosa according to RNA-seq (25). TMEM176A was found frequently methylated in human colorectal, hepatic and esophageal cancers and was suggested to be a tumor suppressor (25–27). The role of TMEM176A in lung cancer remains to be elucidated.

In this study, we found that TMEM176A is frequently methylated in human lung cancer and the expression of TMEM176A is regulated by promoter region methylation. TMEM176A suppressed lung cancer growth both *in vitro* and *in vivo* by inhibiting ERK signaling. Further study found that methylation of TMEM176A sensitized H1299 and H23 cells to AZD0156, an ATM inhibitor, and re-expression of TMEM176A reduced the sensitivity of these cells to AZD0156. Methylation of TMEM176A is a novel synthetic lethality therapeutic marker of ATM inhibitor in human lung cancer.

Materials And Methods

Human tissue samples and cell lines

Primary lung cancer samples (90) were collected from the Chinese PLA General Hospital and 33 primary samples were collected from the tumor hospital of Henan. The median age of the cancer patients was 60 years old (range from 29 to 79). Fifteen cases of normal lung tissue were collected from the Chinese PLA General Hospital. Among 123 cancer samples, only 40 cases were available for paraffin samples with matched cancer and adjacent tissue. All samples were collected following the guidelines approved by the Institutional Review Board of the Chinese PLA General Hospital and the tumor hospital of Henan with written informed consent from patients. Nine lung cancer cell lines (H157, H1563, H727, H358, H446, H460, H23, H1299 and A549) were previously established from primary lung cancer and grown in RPMI-1640 (Invitrogen, Carlsbad, CA, USA) supplemented with 10% fetal bovine serum (Hyclone, Logan, UT) and 1% penicillin/streptomycin solution (Sigma, St. Louis, MO).

5-Aza-2-deoxycytidine and SCH772984 treatment

For methylation regulation analysis, lung cancer cell lines were split to low density (30% confluence) 12 hours before treatment. Cells were treated with 5-Aza-2-deoxycytidine (DAC, Sigma, St. Louis, MO, USA) at a concentration of 2 μM in the growth medium, which was exchanged every 24 hours for a total of 96 hours and cultured at 37°C in a 5% CO2 incubator. At the end of the treatment period, cells were prepared for extraction of total RNA. To verify the role of TMEM176A in ERK signaling, SCH772984, an ERK inhibitor, was added to TMEM176A knocking down H727 cell at 2μm for 24h (MedChemExpress, Monmouth Junction, USA) (28).

RNA isolation and semi-quantitative RT-PCR

Total RNA was extracted using Trizol Reagent (Life Technologies, Carlsbad CA USA). Agarose gel electrophoresis and spectrophotometric analysis were used to detect RNA quality and quantity. First strand cDNA was synthesized according to manufacturer's instructions (Invitrogen, Carlsbad, CA). A total of 5μg RNA was used to synthesize first strand cDNA. The reaction mixture was diluted to 100μl with water, and then 2μl of diluted cDNA was used for 25μl PCR reaction. The PCR primer sequences for TMEM176A were as follows: 5'-GGG AAC AGC CGA CA G TGA T-3' (F) and 5'-GCC AGC GTT AGC AGA GTC CT-3'(R). PCR cycle conditions were as follows: 95°C 5 min, 1 cycle; (95°C 30 s, 60°C 30 s and 72°C 30 s) 32 cycles; 72°C 5 min, 1 cycle. PCR product size is 369bp. GAPDH was amplified for 25 cycles as an internal control. The GAPDH primer sequences were as follows: 5'-GAC CAC AGT CCA TGC CAT CAC-3' (F), and 5'-GTC CAC CAC CCT GTT GCT GTA-3' (R). PCR cycle conditions were as follows: 95°C 5 min, 1 cycle; (95°C 30 s, 63°C 30 s and 72°C 30 s) 25cycles; 72°C 5 min, cycle. PCR product size is 448bp. The amplified PCR products were examined by 2% agarose gels.

DNA extraction, bisulfite modification, methylation specific PCR (MSP)

Genomic DNA from lung cancer cell lines and lung cancer tissue samples were prepared using the proteinase-K method. Normal lymphocyte DNA was prepared from healthy donor blood lymphocytes by proteinase-K method (29). Normal lymphocyte DNA (NL) was used as a control for unmethylation and in vitro methylated DNA (IVD) was used as a methylation control. IVD was prepared using SssI methylase

(New England Biolabs, Ipswich, MA, USA) following the manufacturer's instructions. MSP primers were designed according to genomic sequences inside the CpG islands in the TMEM176A gene promoter region.

MSP primers for TMEM176A were designed -364 to -203bp upstream of the transcription start site (TSS) and synthesized to detect methylated (M) and unmethylated (U) alleles. The detected region has been previously reported to be hypermethylated and associated with low expression (30). MSP primers for TMEM176A were as follows: 5'-GTT TCG TTT AGG TTG CGC GGT TTT TC -3' (MF), 5'-CCA AAA CCG ACG TAC AAA TAT ACG CG-3' (MR); 5'-TGG TTT TGT TTA GGT TGT GTG GTT TTT T-3' (UF),

5'-CAA CCA AAA CCA ACA TAC AAA TAT ACA CA -3' (UR).

PCR cycle conditions were as follows: 95°C 5 min, 1 cycle; (95°C 30 s, 60°C 30 s and 72°C 30 s) 35cycles; 72°C 5 min, 1 cycle.

Bisulfite sequencing (BSSQ) primers encompassed a 231bp region upstream of the TMEM176A transcription start site (-388bp to -157bp) and included the region analyzed by MSP. BSSQ primers were designed as follows:

5'-GAG ACG GTA GAT GTA CGG GT-3' (F);

5'- AAC RAA CRA CCC TAA AAA AAC CC -3' (R). PCR cycle conditions were as follows: 95°C 5 min, 1 cycle; (95°C 30 s, 55°C 30 s and 72°C 30 s) 35cycles; 72°C 5 min, 1 cycle.

Immunohistochemistry

Immunohistochemistry (IHC) was performed in primary lung cancer samples and matched adjacent tissue samples. TMEM176A antibody was diluted to 1:50 (Cat: HPA008770, Sigma, St. Louis, MO, USA). The expression of MMP2, MMP9 and p-ERK1/2 was detected in H1299 cell xenografts. MMP2, MMP9 and p-ERK1/2 antibody was diluted to 1:100, 1:100 (Protein Tech Group, Chicago, IL, USA) and1:400 (Cell Signaling Technology, Danfoss, MA, USA). The procedure was performed as described previously (31). The staining intensity and extent of the staining area were scored using the German semi-quantitative scoring systems as previously described (31-33). Staining intensity of the membrane and/or cytoplasm was characterized as follows: no staining = 0, weak staining = 1, moderate staining = 2, strong staining = 3; the extent of staining was defined as: 0% = 0, 1–24% = 1, 25–49% = 2, 50–74% = 3, 75–100% = 4. The final immune-reactive score (0–12) was determined by multiplying the intensity score by the extent of staining score.

Construction of lentiviral TMEM176A expression vectors and selection of stable expression cells

The human full length TMEM176A cDNA (NM-018487.2) was cloned into the pLenti6 vector. Primers were as follows: 5'- CTT AGG ATC CGC CAC CAT GGG AAC AGC CGAC -3' (F) and 5'- ACT TAG TCG ACC TAG ATT CCA CTC ACT TCC -3'(R). The HEK-293T cell line was maintained in DMEM (Invitrogen, CA, USA)

supplemented with 10% fetal bovine serum. TMEM176A expressing Lentiviral vector was transfected into HEK-293T cells (5.5×10^6 per 100 mm dish) using Lipofectamine 3000 Reagent (Invitrogen, Carlsbad，CA， USA) at a ratio of 1:3 (DNA mass: Lipo mass). Viral supernatant was collected and filtered after 48 hours. H23 and H1299 cells were then infected with viral supernatant. H23 and H1299 cells stably expressing TMEM176A were selected with Blasticidin (Life Technologies, Carlsbad，CA， USA) at concentrations of 6.0μg/ml and 5.0μg/ml for 2 weeks, respectively.

RNA interference assay

Two sets of targeting siRNA for TMEM176A and one set of RNAi negative control duplex sequence are as follows:

SiTMEM176A1 duplex (sense: 5'-GGC UAC UCU UAU UAC AAC ATT-3'; antisense: UGU UGU AAU AAG AGU AGC CTT-3'),

SiTMEM176A2 duplex (sense: 5'-CUG UAC UGC UGG AGA AUG UTT-3'; antisense: 5'-ACA UUC UCC AGC AGU ACA GTT-3'),

SiTMEM176A negative control duplex (SiTMEM176ANC, sense: 5'-ACA UUC UCC AGC AGU ACA GTT-3'; antisense: 5'-ACG UGA CAC GUU CGG AGA ATT-3'). SiTMEM176A2 was found more effective than SiTMEM176A1, and SiTMEM176A2 was applied to further study (GenePharma Co. Shanghai, China).

Cell viability detection

H23 and H1299 cells were seeded into 96-well plates before and after re-expression of TMEM176A at 1×10^3 cells/well. H727 cell were plated into 96-well plates before and after knockdown of TMEM176A at a density of 5×10^3 cells/well. The cell viability was measured by MTT(3-(4,5)-dimethylthiahiazo (-z-y1)-3,5-di- phenytetrazoliumromide) assay at 0h, 24h, 48h, 72h, 96h (KeyGENBiotech, Nanjing, China). Absorbance was measured on a microplate reader (Thermo Multiskan MK3, MA, USA) at a wavelength of 490nm. Each experiment was repeated three times.

H23 and H1299 cells were seeded into 96-well plates at 4×10^3 cells/well and 3×10^3 cells/well irrespectively. The IC50 value was detected by the MTT assay before and after re-expression of TMEM176A. H727 cell were plated into 96-well plates at a density of 8×10^3 cells/well before and after knockdown of TMEM176A. Cells were treated with AZD0156 for 24 hours at 0, 0.001, 0.01.0.1, 1, 10, 100 and 1000 μm/L after seeded for 24 hours (34). Each experiment was repeated for three times.

Colony Formation Assay

TMEM176A unexpressed and re-expressed H23 and H1299 cells were seeded in 6-well plates at a density of 200 cells per well. Before and after knockdown of TMEM176A, H727 cells were seeded into 6-well plates at a density of 300 cells per well. After 2 weeks, cells were fixed with 75% ethanol for 30 min.

Colonies were then stained with 0.5% crystal violet solution and counted. The experiment was performed in triplicate.

Flow cytometry

TMEM176A unexpressed and stably expressed H23 and H1299 cells were starved for 12 hours to synchronize, and cells were re-stimulated with 10% FBS for 24 hours. Cells were fixed with 70% ethanol and treated using the Cell Cycle Detection Kit (KeyGen Biotech, Nanjing, China). Cells were then detected using a FACS Caliber flow cytometer (BD Biosciences, CA, USA). The cell cycle was analyzed also for H727 cells with or without knocking down TMEM176A. Cell phase distribution was analyzed using the Modfit software (Verity Software House, ME, USA).

To increase the sensitivity of apoptosis detection, TMEM176A unexpressed and stably re-expressed H23 and H1299 cells were treated with Doxorubicin at 0.8μg/ml and 0.6μg/ml for 24 hours respectively (35). Apoptosis was also analyzed in H727 cell with or without knockdown of TMEMA176. The cells were prepared using the FITC Annexin V Apoptosis Detection Kit I (BD Biosciences, Franklin Lakes, NJ, USA) following the manufacturer's instructions and then sorted by FACS Calibur (BD Biosciences, Franklin Lakes, NJ, USA). Each experiment was repeated three times.

Transwell assay

For migration study, cells were suspended in 200μl serum-free RPMI 1640 media, and 5×10^4 H23 and 2×10^4 H1299 cells were added to the upper chamber of an 8.0μm pore size transwell apparatus (COSTAR Transwell Corning Incorporated, Tewksbury MA, USA). Cells were stained with crystal violet and counted in three independent high-power fields (×100) after incubation for 16 hours (H23 cells) or 16 hours (H1299). Each experiment was repeated for three times.

For invasion assay, H23 cells (1×10^5) and H1299 cells (5×10^4) were seeded to the upper chamber of a transwell apparatus coated with Matrigel (BD Biosciences, CA, USA) and incubated for 36 hours (H23) and 36 hours (H1299). Each experiment was repeated three times.

Western Blot

Cells were collected 48h after transfection and cell lysates were prepared using ice-cold Tris buffer (20 mmol/L Tris; pH 7.5) containing 137 mmol/L NaCl, 2 mmol/L EDTA, 1% Triton X, 10% glycerol, 50 mmol/L NaF, 1 mmol/L DTT, PMSF, and a protein phosphatases inhibitor (Applygen Tech. Beijing, China). For extracellular signal-regulated kinase (ERK) signaling analysis, cells were starved with serum free medium for 24 h after transfection. These cells were then stimulated with medium containing 10% serum for 60 min before collection. To analyze the sensitivity of AZD0156, cells were exposed to UV 20 mJ/cm2 for 2h before treatment with 0.5μm AZD0156 or ethanol (control), and cells were collected after 24h treatment (36). Western blot was performed as described previously (31).

Primary antibodies were as follows: TMEM176A (Sigma, St. Louis, MO), cleaved caspase-3 (Protein Tech Group, Chicago, IL, USA), MMP2 (Protein Tech Group, Chicago, IL, USA), MMP9 (Protein Tech Group, Chicago, IL, USA), cyclin B1 (Protein Tech Group, Chicago, IL, USA), CDC2 (Protein Tech Group, Chicago, IL, USA), ATM (HuaXingBoChuang, China),γ-H2AX (HuaXingBoChuang, China), p-CHK2(Zhengneng, China), ERK1/2 (Protein Tech Group, Chicago, IL, USA), p-ERK1/2 (Cell Signaling Technology, Danfoss, MA, USA), SAR1A (Protein Tech Group, Chicago, IL, USA) and β-actin (Beyotime Biotech, Nanjing, China).

Lung cancer cell xenograft mouse model

H1299 cell lines stably transfected with plenti6 vector or plenti6-TMEM176A vector (1×10^7 cells diluted in phosphate-buffer saline) were injected subcutaneously into the dorsal left side of 4-week-old female Balb/c nude mice. Each group included six mice. Tumor volume was measured every 4 days. Tumor volume was calculated according to the formula: $V=L\times W^2/2$, in which V represents volume (mm^3), L represents biggest diameter (mm), and W represents smallest diameter (mm). Mice were sacrificed on the 24^{th} day after inoculation and tumors were weighed. All procedures were approved by the Animal Ethics Committee of the Chinese PLA General Hospital.

Data Analysis

RNASeq data for TMEM176A gene expression in the dataset of lung cancer and normal tissues were downloaded from the Cancer Genome Atlas (TCGA) (http://xena.ucsc.edu/, 09/16/2019). Statistical analysis was performed using SPSS 17.0 software (SPSS, Chicago, IL). Chi-square test was used to evaluate the relationship between methylation status and clinicopathological characteristics. The 2-tailed independent samples t-test was applied to determine the statistical significance of the differences between the two experimental groups. Two-sided tests were used to determine the statistical difference, and $P<0.05$ was considered statistically significance.

Results

TMEM176A is frequently methylated in human NSCL cancer and the expression of TMEM176A is regulated by promoter region hypermethylation

The expression of TMEM176A was examined in human lung cancer cells by semi-quantitative RT-PCR. TMEM176A was highly expressed in H727 cell, reduced expression was observed in A549, H446 and H460 cells, and no expression was found in H157, H1563, H358, H1299 and H23 cells (Figure 1A). The promoter region methylation was examined by Methylation-Specific PCR (MSP). Unmethylation was detected in H727 cell, partial methylation was observed in A549, H446 and H460 cells, and complete methylation was found in H157, H1563, H358, H1299 and H23 cells (Figure 1B). These results demonstrate that loss of/reduced expression of TMEM176A was correlated with promoter region methylation.

To further validate that the expression of TMEM176A was regulated by promoter region methylation, lung cancer cells were treated with 5-AZA-2-deoxycytidine. Upon treatment with 5-AZA-2-deoxycytidine, re-expression of TMEM176A was found in H157, H1563, H358, H1299 and H23 cells, increased expression of TMEM176A was observed in A549, H446 and H460 cells, and no expression changes were found in H727 cell before and after treatment (Figure 1A). These results suggest that the expression of TMEM176A is regulated by promoter region methylation in lung cancer cells. To further validate the efficiency of MSP primers and explore the methylation density in lung cancer, sodium bisulfite sequence (BSSQ) was performed in H1299, H23, H727 cells and normal lung tissue samples. Dense methylation was observed in the promoter region of TMEM176A in H1299 and H23 cells, unmethylation was detected in H727 cells and normal lung tissue samples (Figure 1C).

The methylation status of TMEM176A was also detected by MSP in 123 cases of primary human lung cancer and 15 cases of non-cancerous lung tissue samples. TMEM176A was methylated in 53.66% (67/123) of human primary lung cancer, and no methylation was found in non-cancerous lung tissue samples (Figure 2A). No association was found between TMEM176A methylation and age, gender, alcohol abuse, smoking, tumor size, lymph node metastasis, differentiation and TNM stage (table1, all P >0.05).

The expression of TMEM176A was evaluated by immunohistochemistry in 40 cases of available matched lung cancer and adjacent tissue samples. TMEM176A staining was found mainly in cytoplasm and cell membranes (Figure 2B). The expression levels of TMEM176A were reduced in cancer compared to adjacent tissue samples (Figure 2C, Student's t-distribution (t-test), $P < 0.05$). Lower level expression of TMEM176A was found in 35 cases of cancer tissue. Among the 35 cases that had reduced expression of TMEM176A, 20 cases were methylated. These data indicate that the expression of TMEM176A is regulated by promoter region methylation in human primary lung cancer.

The Cancer Genome Atlas (TCGA) database was employed to further validate that the expression of TMEM176A is regulated by promoter region methylation. TMEM176A mRNA expression and promoter region methylation data were extracted from the TCGA database (http://xena.ucsc.edu/). Methylation of TMEM176A (cg19336959) was analyzed by Illumina Infinium Human Methylation 450 (HM450). In the 457 cases of lung adenocarcinoma samples and 372 cases of lung squamous carcinoma samples, reduced expression of TMEM176A was associated with promoter region hypermethylation (Figure 2E, 2F). These data further suggested that the expression of TMEM176A is regulated by promoter region methylation.

TMEM176A inhibits lung cancer cells proliferation

MTT and colony formation assays were used to evaluate the effects of TMEM176A on cell proliferation. TMEM176A stably expressed cells were established by transfection assay and TMEM176A highly expressed cells were knocked down by siRNA. The OD values were 0.648 ± 0.006 *vs.* 0.527 ± 0.005 in H23 cells (P <0.001) and 0.878 ± 0.010 *vs.* 0.700 ± 0.008 (P <0. 001) in H1299 cells before and after restoration of TMEM176A expression (Figure 3A). The OD values were reduced significantly after

restoration of TMEM176A expression in H23 and H1299 cells (both P<0.001). The OD values were 0.550 ± 0.040 *vs.* 0.673 ± 0.025 (P< 0.001) in H727 before and after knockdown of TMEM176A (Figure 3A). The OD values increased significantly after knockdown of TMEM176A expression in H727 cell (P<0.001). These results demonstrated that TMEM176A inhibits cell proliferation in lung cancer cells. The clone numbers were 99.6 ± 3.5 *vs.* 42.0 ± 7.5 (P< 0.001) in H23 cells and 128.7 ± 5.9 *vs.* 47.7 ± 5.7 in H1299 cells (P <0.01) before and after restoration of TMEM176A expression (Figure 3B). The clone numbers were 26 ± 7.9 *vs.* 71.3 ± 11.3 in H727 cells (P <0.01) before and after knockdown of TMEM176A (Figure 3B). These data suggest that TMEM176A suppresses cell growth in lung cancer.

TMEM176A induces lung cancer cells apoptosis

The effect of TMEM176A on apoptosis was analyzed by flow cytometry. Under doxorubicin treatment, the ratios of apoptotic cells in TMEM176A un-expressed and re-expressed cells were 3.20 ± 0.01% *vs.* 29.80 ± 0.03% in H23 cells, and 0.80 ± 0.00% *vs.* 2.10 ± 0.00% in H1299 cells. The ratio of apoptotic cells increased significantly after re-expression of TMEM176A (all P<0.05, Figure 3C). In H727 cell, the ratios of apoptotic cells were 4.17 ± 0.00% *vs.* 2.30 ± 0.01% before and after knockdown of TMEM176A. The ratio of apoptotic cells decreased significantly after knockdown of TMEM176A (P<0.05, Figure 3C). To further validate the effect of TMEM176A on apoptosis, cleaved caspase-3 expression was analyzed in lung cancer cells. The levels of cleaved caspase-3 increased after re-expression of TMEM176A in H23 and H1299 cells and decreased after knockdown of TMEM176A in H727 cell (Figure 3G). These results demonstrate that TMEM176A induces apoptosis in lung cancer cells.

TMEM176A induces G2/M phase arrest in lung cancer cells

To evaluate the effect of TMEM176A on the cell cycle, flow cytometry was employed. The percentage of cell phases in TMEM176A unexpressed and re-expressed H23 cell lines was 56.95 ± 0.07% vs. 56.16 ± 0.06% in G0/G1 phase, 29.35 ± 0.16% vs. 23.46 ± 0.30% in S phase, and 13.70 ± 0.19% vs. 20.38 ± 0.26% in G2/M phase. The G2/M phase was increased significantly after re-expression of TMEM176A (P < 0.001, Figure 3D). In H1299 cells, the percentage of the cell phase was 70.66 ± 1.10% vs. 63.28% ± 0.54% in G0/G1 phase, 21.97 ± 0.51% vs. 18.72 ± 0.45% in S phase, and 7.37 ± 0.80% vs. 18.00 ± 0.24% in G2/M phase before and after restoration of TMEM176A expression. The G2/M phase was increased significantly after re-expression of TMEM176A in H1299 cells (P < 0.001, Figure 3D). The effect of TMEM176A on cell cycle was further validated by knocking down TMEM176A in TMEM176A highly expressed H727 cells. The distribution of cell phases was 45.86 ± 0.50% vs. 50.46 ± 0.66% in G0/G1 phase, 34.95 ± 0.78% vs. 40.75 ± 0.32% in S phase, and 19.19 ± 0.61% vs. 9.02 ± 0.13% in G2/M phase. The G2/M phase was significantly reduced by knocking down TMEM176A in H727 cells (P < 0.001, Figure 3D). Above results suggest that TMEM176A induced G2/M phase arrest. The levels of cyclinB1 and CDC2 were also detected by western blot. As shown in Figure 3G, the levels of cyclinB1 and CDC2 were reduced after re-expression of TMEM176A in H23 and H1299 cells. The levels of cyclinB1 and CDC2 were increased after knockdown of TMEM176A in H727 cells. These results further suggest that TMEM176A induces G2/M phase arrest in human lung cancer cells.

TMEM176A inhibits lung cancer cellmigrationand invasion

To evaluate the effects of TMEM176A on cell migration and invasion, transwell assays were used. The numbers of migration cells were 431.5 ± 8.22 *vs.* 98.0 ± 4.83 in H23 cells and 562.0 ± 15.03 *vs.* 285.0 ± 3.46 in H1299 cells before and after restoration of TMEM176A expression. The number of migration cells decreased significantly after re-expression of TMEM176A in H23 and H1299 cells (both $P < 0.001$, Figure 3E). The numbers of invasion cells were 434.8 ± 18.60 *vs.* 133.3 ± 5.40 in H23 cells and 306.7 ± 48.21 *vs.* 152.0 ± 7.30 in H1299 cells before and after restoration of TMEM176A expression. The cell number decreased significantly after re-expression of TMEM176A in H23 and H1299 cells (both $P< 0.001$, Figure 3F). These results suggest that TMEM176A suppresses lung cancer cell migration and invasion. To further explore the mechanism of TMEM176A on cell migration and invasion, MMP2 and MMP9 expression were measured by Western blot. The expression levels of MMP2 and MMP9 were reduced after re-expression of TMEM176A in H23 and H1299 cells. These results suggest that TMEM176A inhibits cell invasion in lung cancer cells (Figure 3G). As H727 is carcinoid cell and the invasive and migration ability are very poor. Therefore, the transwell assay was not performed.

TMEM176A inhibits ERK signaling pathway in lung cancer cells

TMEM176A was found involved in ERK signaling in our previous study in hepatic cancer (26). The function of TMEM176A in ERK signaling was analyzed in human lung cancer. The levels of total ERK1/2 and phosphorylated ERK1/2 (p-ERK1/2) were detected by Western blot in lung cancer cells with or without TMEM176A expression. As shown in Figure 4A, though the levels of ERK1/2 were not apparent different before and after re-expression of TMEM176A in H23 and H1299 cells, the levels of p-ERK1/2 were reduced after re-expression of TMEM176A in H23 and H1299 cells. The levels of ERK1/2 in TMEM176A highly expressed H727 cells were similar to TMEM176A knocking down cells by siRNA, while the levels of p-ERK1/2 were increased after knockdown of TMEM176A in H727 cells. These results suggest that TMEM176A inhibits ERK signaling in lung cancer cells.

To further validate above results, MTT assay and ERK1/2 signaling inhibitor (SCH772984) was employed. The OD values were 0.692 ± 0.011, 0.650 ± 0.011, 0.848 ± 0.019 and 0.614± 0.025 in control group, control group plus SCH772984 treatment, siTMEM176A group and siTMEM176A plus SCH772984 treatment group in H727 cells, respectively. No significant difference was found between control group, control group plus SCH772984 and siTMEM176A plus SCH772984 treatment group (both $P> 0.05$) in H727 cells. While, the OD value is reduced significantly in siTMEM176A plus SCH772984 treatment group compared to siTMEM176A group in H727 cells ($P < 0.001$, Figure 4B). P-ERK1/2 is significantly reduced in plus SCH772984 treatment group (Figure 4C). Above results further validated that TMEM176A inhibits ERK signaling in lung cancer.

Epigenetic silencing of TMEM176A sensitized lung cancer cells to AZD0156

ERK signaling was reported to be a positive regulator of ATM-dependent DNA homologous recombination repair (HR)(37). We found that TMEM176A inhibits ERK signaling in human lung cancer. To further

explore the possibility of synthetic lethality effect of TMEM176A methylation and ATM inhibitor in human lung cancer, we tested the sensitivity of TMEM176A unexpressed and re-expressed H1299 cells and H23 cells to AZD0156. The IC50 of AZD0156 was 1.38 ± 0.74 versus 4.00 ± 0.70 μM in TMEM176A unexpressed and re-expressed H23 cells, and 1.88 ± 0.56 versus 4.76 ± 0.70 in TMEM176A unexpressed and re-expressed H1299 cells, respectively. The IC50 was reduced significantly after silencing of TMEM176A by promoter region hypermethylation in human lung cancer cells (all $P < 0.05$, Figure 4D). The effect was further validated by siRNA knocking down in TMEM176A highly expressed lung cancer cells. The IC50 was 7.61 ± 0.81 versus 4.39 ± 0.74 μM in H727 cells before and after knockdown of TMEM176A. The level of IC50 was reduced significantly after knockdown of TMEM176A ($P < 0.05$, Figure 4D). Above results suggest that silencing or knockdown of TMEM176A expression sensitized lung cancer cells to ATM inhibitor. To further validate the effect of TMEM176A on DDR, the levels of ATM, p-CHK2, γ-H2AX and RAD51 were detected by Western blot in TMEM176A unexpressed and re-expressed lung cancer cells. The protein of p-CHK2 is the key factor downstream of ATM pathway. As shown in Figure 4E, p-CHK2, the active form key downstream factor of ATM pathway was detected before and after re-expression of TMEM176A in H23 and H1299 cells under UV treatment. The levels of p-CHK2 were reduced after re-expression of TMEM176A. After exposed to UV for 2 hours, lung cancer cells were treated with AZD0156 for 24 hours. The levels of γ-H2AX were higher in TMEM176A unexpressed H23 and H1299 cells compared to re-expressed H23 and H1299 cells. The levels of RAD51 were lower in TMEM176A unexpressed H23 and H1299 cells compared to re-expressed H23 and H1299 cells (Figure 4E). The levels of ATM, p-CHK2,γ-H2AX and RAD51 were detected in TMEM176A highly expressed H727 cells before and after siRNA knocking down. The levels of p-CHK2 were increased after knockdown of TMEM176A in H727 cells under UV treatment (Figure 4E). The levels of γ-H2AX were increased and the levels of RAD51 were reduced after knocking down of TMEM176A in H727 cells (Figure 4E).

As the significant overlap between the ATR (AT and Rad3-related protein) and ATM pathway, we analyzed the effect of ATR inhibitor (AZD6738) on TMEM176A expressed and unexpressed lung cancer cells. The IC50 of AZD6738 was 10.38 ± 0.60 versus 9.91 ± 0.64 μM in TMEM176A unexpressed and re-expressed H23 cells, and 12.89 ± 0.15 versus 11.89 ± 0.25 μM in TMEM176A unexpressed and re-expressed H1299 cells, respectively (all P 0.05). There is no significant difference between TMEM176A unexpressed and re-expressed cancer cells. The results suggest that TMEM176A is not involved in ATR pathway through ERK signaling.

TMEM176A suppresses human lung cancer cell xenograft growth by inhibiting ERK signaling

To further evaluate the effect of TMEM176A in human lung cancer, TMEM176A unexpressed and re-expressed H1299 cells were used to establish xenograft mouse models (Figure 5A). The tumor volume was 983.32 ± 101.76 *vs.* 216.06 ± 86.96 mm^3 in TMEM176A unexpressed and re-expressed H1299 cell xenografts (Figure 5B). The tumor volume was reduced significantly in TMEM176A re-expressed H1299 cell xenograft mice ($P<0.001$). The tumor weight was 0.68 ± 0.11g *vs.* 0.20 ± 0.07g in TMEM176A unexpressed and re-expressed H1299 cell xenograft mice (Figure 5C). The tumor weight was reduced significantly in TMEM176A re-expressed H1299 cells xenograft mice ($P<0.001$). These results indicate

that TMEM176A suppresses lung cancer cell growth *in vivo*. To further validate the effect of TMEM176A on tumor metastasis, the expression of MMP2 and MMP9 were examined by IHC in xenograft tumors. The expression levels of MMP2 and MMP9 were decreased in TMEM176A re-expressed H1299 cell xenografts compared to TMEM176A un-expressed H1299 cells (Figure 5D). To further validate that TMEM176A inhibits ERK signaling *in vivo*, the levels of p-ERK1/2 was detected by IHC staining in TMEM176A unexpressed and re-expressed H1299 cell xenografts. The levels of p-ERK1/2 decreased obviously in TMEM176A re-expressed H1299 cell xenografts (Figure 5D).

Discussion

TMEM176A is located in human chromosome 7q36.1, a region where there is a frequent loss of heterozygosity in human cancers (38, 39). By RNA-seq analysis, we found that the expression of TMEM176A was reduced in human colorectal cancer (25). TMEM176A was found frequently methylated in human colorectal, esophageal and hepatic cancers in our previous studies. TMEM176A was demonstrated to be a potential tumor suppressor in these cancers (25-27). While, a recently report suggest that the expression of TMEM176A was increased in primary human glioblastoma, and TMEM176A promoted glioblastoma cell proliferation by activating ERK signaling. They also found that both TMEM176A and TMEM176B were increased expression in glioblastoma (40). The expression pattern is different from other cancers, and no correlation was found between TMEM176A and TMEM176B expression in other cancers (25-27). Drujont et al. found that the expression of TMEM176A was increased in TMEM176b-/- cells compared with wild type cells of Th17 in mice (41). The expression pattern of TMEM176A and TMEM176B are possibly discrepant in different tissues. TMEM176A and TMEM176B may play different roles in varies microenvironment. TMEM176B was not expressed in most of human lung cancer cells (data not show). In this study, we found that TMEM176A is frequently methylated in human lung cancer and the expression of TMEM176A is regulated by promoter region methylation. Methylation of TMEM176A may serve as a potential lung cancer diagnostic marker. TMEM176A inhibits cell proliferation, invasion, migration, colony formation, induces G2/M phase arrest and apoptosis in lung cancer. TMEM176A suppresses H1299 lung cancer cell xenografts growth in mice. Further study found that TMEM176A suppresses lung cancer growth by inhibiting ERK signaling both *in vitro* and *in vivo*.

Even through a lot of targeting “epigenetic machinery” inhibitors are ongoing clinical trials (42). There are many challenges to be resolved for efficient use of epidrugs in the treatment of human cancer, including the lack of specificity, disappointing success in solid tumors and the acquisition of drug chemo-resistance leading to higher risk of tumor relapse. As no specific clinical detective marker of histone modifications in tumor detection, the efficiency of targeting histone modifier therapy remains very limited(10). Epigenetic-based synthetic lethal therapy may be more specific and efficient. Beyond ‘BRCAness’, aberrant epigenetic changes are more suitable for ‘synthetic lethality’ and provide new opportunities for cancer therapy (14, 15). The role of ERK was clearly defined as a positive regulator of HR and HR is the most important DDR in late S and G2/M phases of the cell cycle (37). ATM and ATR are two major kinases to take part in DDR, and ATM specifically regulates HR(43). TMEM176A induced G2/M

arrest in lung cancer cells. Thus, we analyzed the role of TMEM176A in ATM pathway. Our study demonstrated that methylation of TMEM176A sensitized H1299 and H23 cells to AZD0156, and restoration of TMEM176A expression decreased their sensitivities to AZD0156. The results suggest that methylation of TMEM176A is a sensitive marker of ATM inhibitor for lung cancer cells. There is considerable overlap of the phosphorylation substrates of both ATR and ATM. Then, we detected the sensitivity of ATR inhibitor, AZD6738, TMEM176A expressed and unexpressed lung cancer cells. No difference was found between TMEM176A expressed and unexpressed lung cancer cells for AZD6738. No synthetic effect was found between ATR inhibitor and defect of TMEM176A. Our results suggest that methylation of TMEM176A is a synthetic lethal marker for ATM inhibitor in lung cancer. Figure 6 illustrates the schematic synthetic lethality between TMEM176A methylation and ATM inhibitor in lung cancer.

Conclusions

In conclusion, TMEM176A suppresses lung cancer growth both *in vitro* and *in vivo* by inhibiting ERK signaling pathway. TMEM176A is a potential tumor suppressor in human lung cancer. Methylation of TMEM176A is a potential diagnostic marker and a novel synthetic lethal therapeutic marker for ATM inhibitor in human lung cancer.

Abbreviations

ATM: ataxia telangiectasia mutated; BSSQ: Bisulfite sequencing; ATR: AT and Rad3-related protein; DAC: 5-Aza-2'-deoxycytidine; HM450: Illumina Infinium Human Methylation 450; IHC: Immunohistochemistry; MSP: Methylation specific PCR; RT-PCR: Reverse transcription PCR; TCGA: The Cancer Genome Atlas; TSS: Transcription start sites; GAPDH: Glyceraldehyde-3-phosphate dehydrogenase; IVD: In vitro-methylated DNA; NL: Normal lymphocyte DNA; LUAD: lung adenocarcinoma; LUSC: lung squamous cell carcinoma;

Declarations

Acknowledgments

Not applicable.

Authors' contributions

HL performed the research and analyzed the data. HL and MG wrote the manuscript. MG made substantial contributions to the conception and design of the study, WY, TH, FZ, HL and JH (James G. Herman) provided manuscript and experimental advice. LH supervised the study. All authors read and approved the final manuscript.

Funding

This work was supported by grants from National Key Research and Development Programme of China (2018YFA0208902); National Science Foundation of China (NSFC No. U1604281, 81672138); National Basic Research Program of China (973 Program No. 2012CB934002, 863 Program No. 2012AA02A203, 2012AA02A209); National Key Scientific Instrument Special Programme of China (Grant No. 2011YQ03013405); Beijing Science Foundation of China (BJSFC No. 7171008).

Availability of data and materials

The material supporting the conclusion of this study has been included within the article.

Ethics approval and consent to participate

All samples were collected following the guidelines approved by the Institutional Review Board of the Chinese PLA General Hospital and the tumor hospital of Henan with written informed consent from patients.

Consent for publication

Not applicable.

Competing interests:

The authors declare no conflict of interest.

Author details

1. Faculty of Environmental and Life Science, Beijing University of Technology, Beijing 100124, China.
2. Department of Gastroenterology & Hepatology, Chinese PLA General Hospital, #28 Fuxing Road, Beijing 100853, China.
3. Department of Pathology, Characteristic Medical Center of the Chinese People's Armed Police Force, Tianjin, 300162, People's Republic of China.
4. Department of Thoracic Surgery, Anyang Tumor Hospital, Anyang 455000.
5. The Hillman Cancer Center, University of Pittsburgh Cancer Institute, 5117 Centre Avenue, Suite 2.18/Research, Pittsburgh, PA 15213, USA.
6. Henan Key Laboratory for Esophageal Cancer Research, Zhengzhou University, 40 Daxue Road, Zhengzhou, Henan, 450052, China.
7. State Key Laboratory of Kidney Diseases, Chinese PLA General Hospital, #28 Fuxing Road, Beijing, 100853, China.

References

1. Bray F, Ferlay J, Soerjomataram I, Siegel RL, Torre LA, Jemal A. Global cancer statistics 2018: GLOBOCAN estimates of incidence and mortality worldwide for 36 cancers in 185 countries. CA

Cancer J Clin. 2018;68(6):394-424.
2. Reck M, Rabe KF. Precision Diagnosis and Treatment for Advanced Non-Small-Cell Lung Cancer. The New England journal of medicine. 2017;377(9):849-61.
3. Corrales L, Rosell R, Cardona AF, Martin C, Zatarain-Barron ZL, Arrieta O. Lung cancer in never smokers: The role of different risk factors other than tobacco smoking. Critical reviews in oncology/hematology. 2020;148:102895.
4. Brock MV, Hooker CM, Ota-Machida E, Han Y, Guo M, Ames S, et al. DNA methylation markers and early recurrence in stage I lung cancer. The New England journal of medicine. 2008;358(11):1118-28.
5. Guo M, Ren J, House MG, Qi Y, Brock MV, Herman JG. Accumulation of promoter methylation suggests epigenetic progression in squamous cell carcinoma of the esophagus. Clin Cancer Res. 2006;12(15):4515-22.
6. Yuan M, Huang LL, Chen JH, Wu J, Xu Q. The emerging treatment landscape of targeted therapy in non-small-cell lung cancer. Signal transduction and targeted therapy. 2019;4:61.
7. Guo M, Liu S, Lu F. Gefitinib-sensitizing mutations in esophageal carcinoma. The New England journal of medicine. 2006;354(20):2193-4.
8. Herbst RS, Morgensztern D, Boshoff C. The biology and management of non-small cell lung cancer. Nature. 2018;553(7689):446-54.
9. Lim ZF, Ma PC. Emerging insights of tumor heterogeneity and drug resistance mechanisms in lung cancer targeted therapy. Journal of hematology & oncology. 2019;12(1):134.
10. Guo M, Peng Y, Gao A, Du C, Herman JG. Epigenetic heterogeneity in cancer. Biomarker research. 2019;7:23.
11. Guo M, Alumkal J, Drachova T, Gao D, Marina SS, Jen J, et al. CHFR methylation strongly correlates with methylation of DNA damage repair and apoptotic pathway genes in non-small cell lung cancer. Discovery medicine. 2015;19(104):151-8.
12. Yu Y, Yan W, Liu X, Jia Y, Cao B, Yu Y, et al. DACT2 is frequently methylated in human gastric cancer and methylation of DACT2 activated Wnt signaling. American journal of cancer research. 2014;4(6):710-24.
13. Dolsten M, Søgaard M. Precision medicine: an approach to R&D for delivering superior medicines to patients. Clinical and translational medicine. 2012;1(1):7.
14. Gao A, Guo M. Epigenetic based synthetic lethal strategies in human cancers. Biomarker research. 2020;8:44.
15. Hu Y, Guo M. Synthetic lethality strategies: Beyond BRCA1/2 mutations in pancreatic cancer. Cancer science. 2020;111(9):3111-21.
16. McLornan DP, List A, Mufti GJ. Applying synthetic lethality for the selective targeting of cancer. The New England journal of medicine. 2014;371(18):1725-35.
17. Bryant HE, Schultz N, Thomas HD, Parker KM, Flower D, Lopez E, et al. Specific killing of BRCA2-deficient tumours with inhibitors of poly(ADP-ribose) polymerase. Nature. 2005;434(7035):913-7.

18. Farmer H, McCabe N, Lord CJ, Tutt AN, Johnson DA, Richardson TB, et al. Targeting the DNA repair defect in BRCA mutant cells as a therapeutic strategy. Nature. 2005;434(7035):917-21.
19. Hu Y, Wen Z, Liu S, Cai Y, Guo J, Xu Y, et al. Ibrutinib suppresses intracellular mycobacterium tuberculosis growth by inducing macrophage autophagy. The Journal of infection. 2020;80(6):e19-e26.
20. Gehrau R, Maluf D, Archer K, Stravitz R, Suh J, Le N, et al. Molecular pathways differentiate hepatitis C virus (HCV) recurrence from acute cellular rejection in HCV liver recipients. Molecular medicine (Cambridge, Mass). 2011;17(7-8):824-33.
21. Nakajima H, Takenaka M, Kaimori JY, Nagasawa Y, Kosugi A, Kawamoto S, et al. Gene expression profile of renal proximal tubules regulated by proteinuria. Kidney international. 2002;61(5):1577-87.
22. Zuccolo J, Deng L, Unruh TL, Sanyal R, Bau JA, Storek J, et al. Expression of MS4A and TMEM176 Genes in Human B Lymphocytes. Front Immunol. 2013;4:195.
23. Condamine T, Le Texier L, Howie D, Lavault A, Hill M, Halary F, et al. Tmem176B and Tmem176A are associated with the immature state of dendritic cells. J Leukoc Biol. 2010;88(3):507-15.
24. Grunin M, Hagbi-Levi S, Rinsky B, Smith Y, Chowers I. Transcriptome Analysis on Monocytes from Patients with Neovascular Age-Related Macular Degeneration. Sci Rep. 2016;6:29046.
25. Gao D, Han Y, Yang Y, Herman JG, Linghu E, Zhan Q, et al. Methylation of TMEM176A is an independent prognostic marker and is involved in human colorectal cancer development. Epigenetics. 2017;12(7):575-83.
26. Li H, Zhang M, Linghu E, Zhou F, Herman JG, Hu L, et al. Epigenetic silencing of TMEM176A activates ERK signaling in human hepatocellular carcinoma. Clin Epigenetics. 2018;10(1):137.
27. Wang Y, Zhang Y, Herman JG, Linghu E, Guo M. Epigenetic silencing of TMEM176A promotes esophageal squamous cell cancer development. Oncotarget. 2017;8(41):70035-48.
28. Patel JD, Paz-Ares L, Zinner RG, Barlesi F, Koustenis AG, Obasaju CK. Pemetrexed Continuation Maintenance Phase 3 Trials in Nonsquamous, Non-Small-Cell Lung Cancer: Focus on 2-Year Overall Survival and Continuum of Care. Clinical lung cancer. 2018;19(6):e823-e30.
29. Zheng R, Gao D, He T, Zhang M, Zhang X, Linghu E, et al. Methylation of DIRAS1 promotes colorectal cancer progression and may serve as a marker for poor prognosis. Clin Epigenetics. 2017;9:50.
30. Wang Y ZY, Herman J. G, Linghu E, Guo M. Epigenetic silencing of TMEM176A promotes esophageal squamous cell cancer development. Oncotarget. 2017;8(41):70035-48.
31. Yan W, Wu K, Herman JG, Brock MV, Fuks F, Yang L, et al. Epigenetic regulation of DACH1, a novel Wnt signaling component in colorectal cancer. Epigenetics. 2013;8(12):1373-83.
32. Jia Y, Yang Y, Liu S, Herman JG, Lu F, Guo M. SOX17 antagonizes WNT/beta-catenin signaling pathway in hepatocellular carcinoma. Epigenetics. 2010;5(8):743-9.
33. Cui Y GD, Linghu E, Zhan Q, Chen R, Brock M V, Herman J G , Guo M. Epigenetic changes and functional study of HOXA11 in human gastric cancer. Epigenomics. 2015;7(2):201-13.

34. Brown JS, O'Carrigan B, Jackson SP, Yap TA. Targeting DNA Repair in Cancer: Beyond PARP Inhibitors. Cancer discovery. 2017;7(1):20-37.
35. Yang MC, Lin RW, Huang SB, Huang SY, Chen WJ, Wang S, et al. Bim directly antagonizes Bcl-xl in doxorubicin-induced prostate cancer cell apoptosis independently of p53. Cell Cycle. 2016;15(3):394-402.
36. Hegedűs C, Boros G, Fidrus E, Kis GN, Antal M, Juhász T, et al. PARP1 Inhibition Augments UVB-Mediated Mitochondrial Changes-Implications for UV-Induced DNA Repair and Photocarcinogenesis. Cancers. 2019;12(1).
37. Sarah E. Golding ER, Steven Neill, Paul Dent, Lawrence F. Povirk, and Kristoffer Valerie. ERK regulates ataxia telangiectasia mutated, homologous recombination repair, and the DNA damage response. Cancer Res. 2007.
38. Riegman PH, Burgart LJ, Wang KK, Wink-Godschalk JC, Dinjens WN, Siersema PD, et al. Allelic imbalance of 7q32.3-q36.1 during tumorigenesis in Barrett's esophagus. Cancer Res. 2002;62(5):1531-3.
39. Kimmel RR, Zhao LP, Nguyen D, Lee S, Aronszajn M, Cheng C, et al. Microarray comparative genomic hybridization reveals genome-wide patterns of DNA gains and losses in post-Chernobyl thyroid cancer. Radiat Res. 2006;166(3):519-31.
40. Liu Z, An H, Song P, Wang D, Li S, Chen K, et al. Potential targets of TMEM176A in the growth of glioblastoma cells. OncoTargets and therapy. 2018;11:7763-75.
41. Drujont L, Lemoine A, Moreau A, Bienvenu G, Lancien M, Cens T, et al. RORgammat+ cells selectively express redundant cation channels linked to the Golgi apparatus. Sci Rep. 2016;6:23682.
42. Yan W, Herman JG, Guo M. Epigenome-based personalized medicine in human cancer. Epigenomics. 2016;8(1):119-33.
43. Morrison C, Sonoda E, Takao N, Shinohara A, Yamamoto K, Takeda S. The controlling role of ATM in homologous recombinational repair of DNA damage. The EMBO journal. 2000;19(3):463-71.

Figures

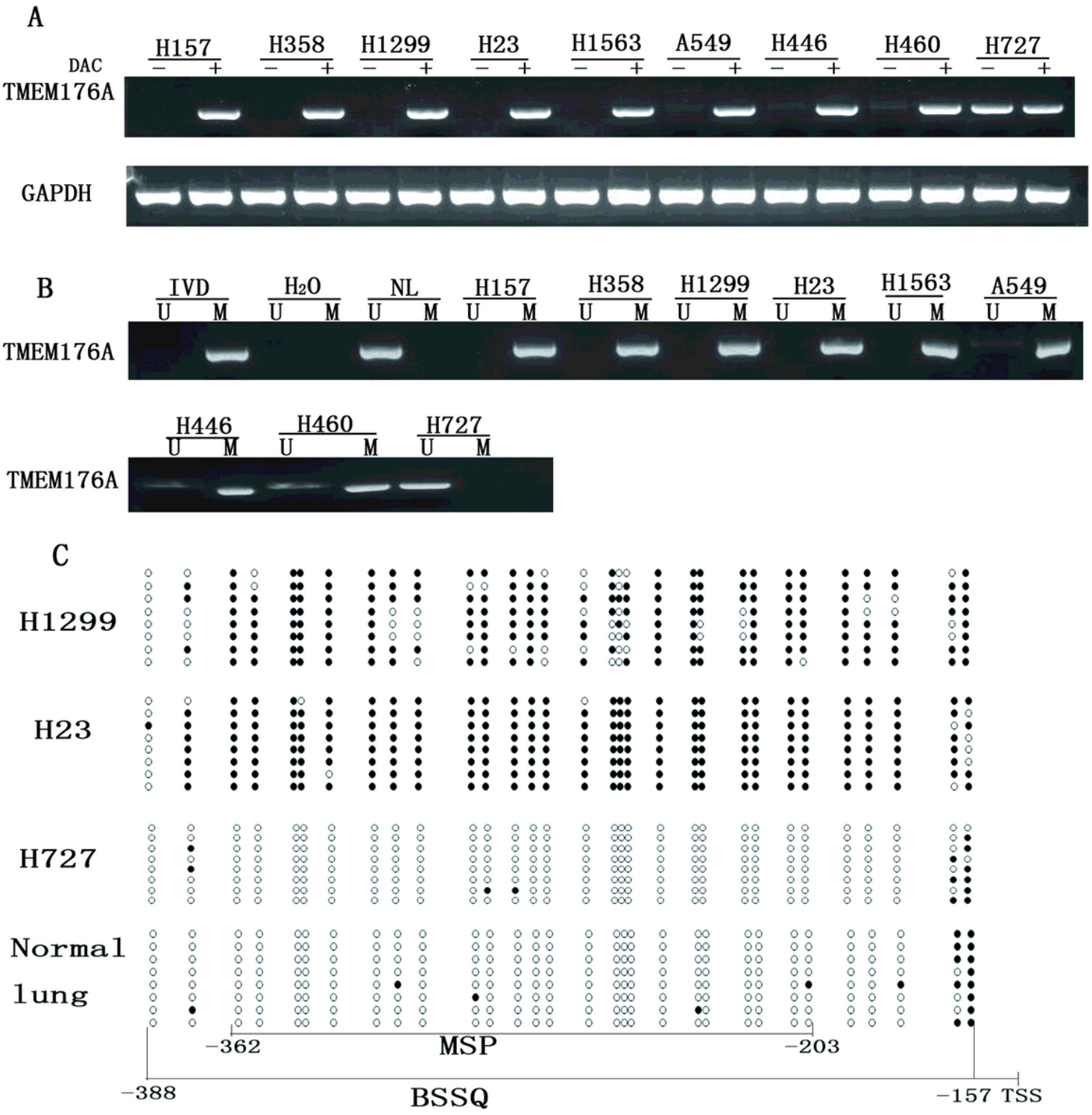

Figure 1

TMEM176A expression and methylation status in human lung cancer cells A. Semi-quantitative RT-PCR shows TMEM176A expression levels in lung cancer cell lines. H157, H358, H1299, H23, H1563, A549, H446, H460 and H727 are lung cancer cells. DAC: 5-aza-2-deoxycytidine; GAPDH: internal control; (-): absence of DAC; (+): presence of DAC. B. MSP results of TMEM176A in lung cancer cell lines. U: unmethylated alleles; M: methylated alleles; IVD: in vitro methylated DNA, serves as methylation control;

NL: normal peripheral lymphocytes DNA, serves as unmethylated control; H2O: double distilled water. C. BSSQ results of TMEM176A in H1299, H23, H727 cells and normal lung. MSP PCR product size was 159bp and bisulfite sequencing focused on a 231bp region of the CpG island (from -388 to -157) around the TMEM176A transcription start site. Filled circles: methylated CpG sites, open circles: unmethylated CpG sites. TSS: transcription start site.

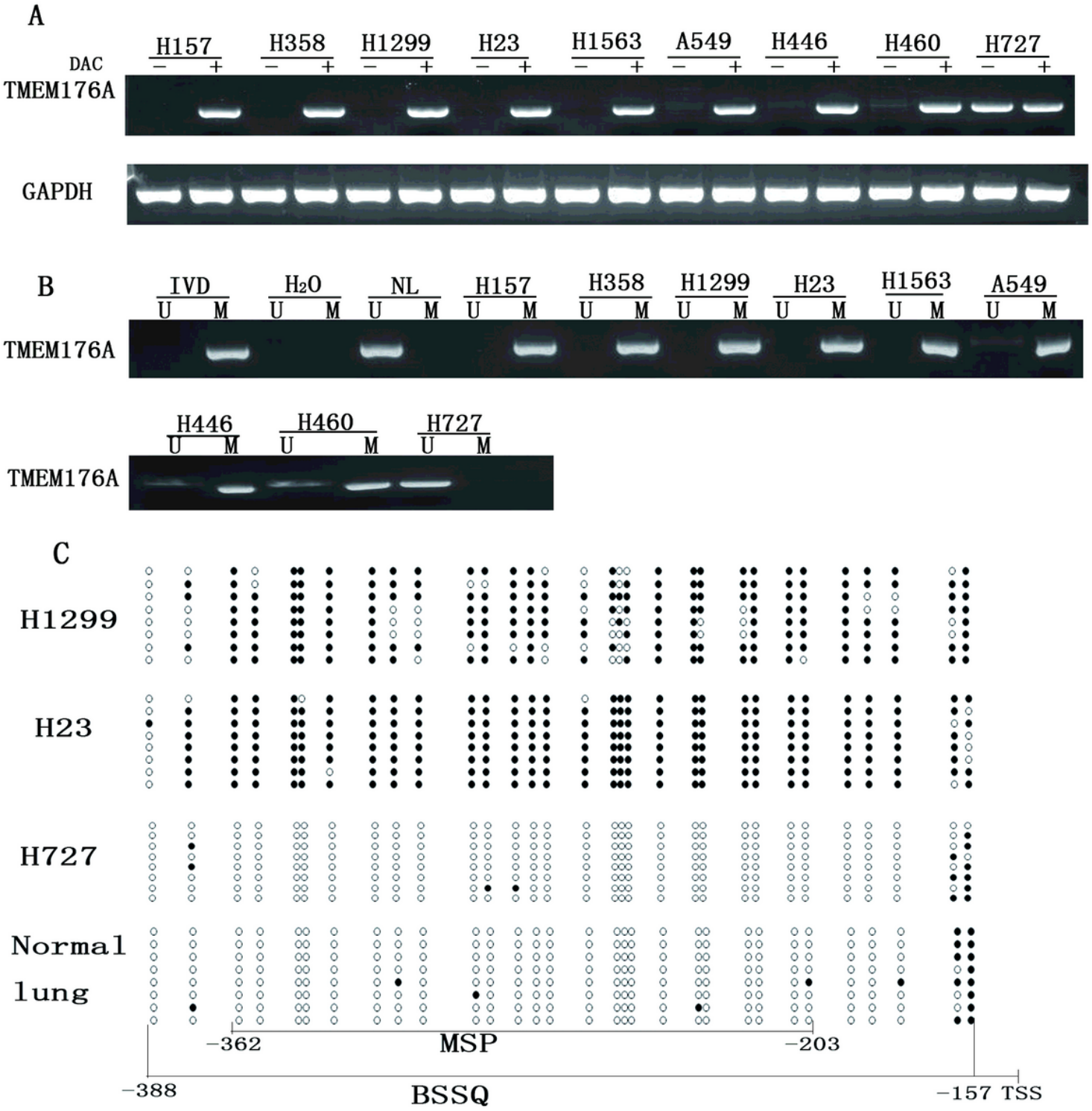

Figure 1

TMEM176A expression and methylation status in human lung cancer cells A. Semi-quantitative RT-PCR shows TMEM176A expression levels in lung cancer cell lines. H157, H358, H1299, H23, H1563, A549, H446, H460 and H727 are lung cancer cells. DAC: 5-aza-2-deoxycytidine; GAPDH: internal control; (-): absence of DAC; (+): presence of DAC. B. MSP results of TMEM176A in lung cancer cell lines. U: unmethylated alleles; M: methylated alleles; IVD: in vitro methylated DNA, serves as methylation control; NL: normal peripheral lymphocytes DNA, serves as unmethylated control; H2O: double distilled water. C. BSSQ results of TMEM176A in H1299, H23, H727 cells and normal lung. MSP PCR product size was 159bp and bisulfite sequencing focused on a 231bp region of the CpG island (from -388 to -157) around the TMEM176A transcription start site. Filled circles: methylated CpG sites, open circles: unmethylated CpG sites. TSS: transcription start site.

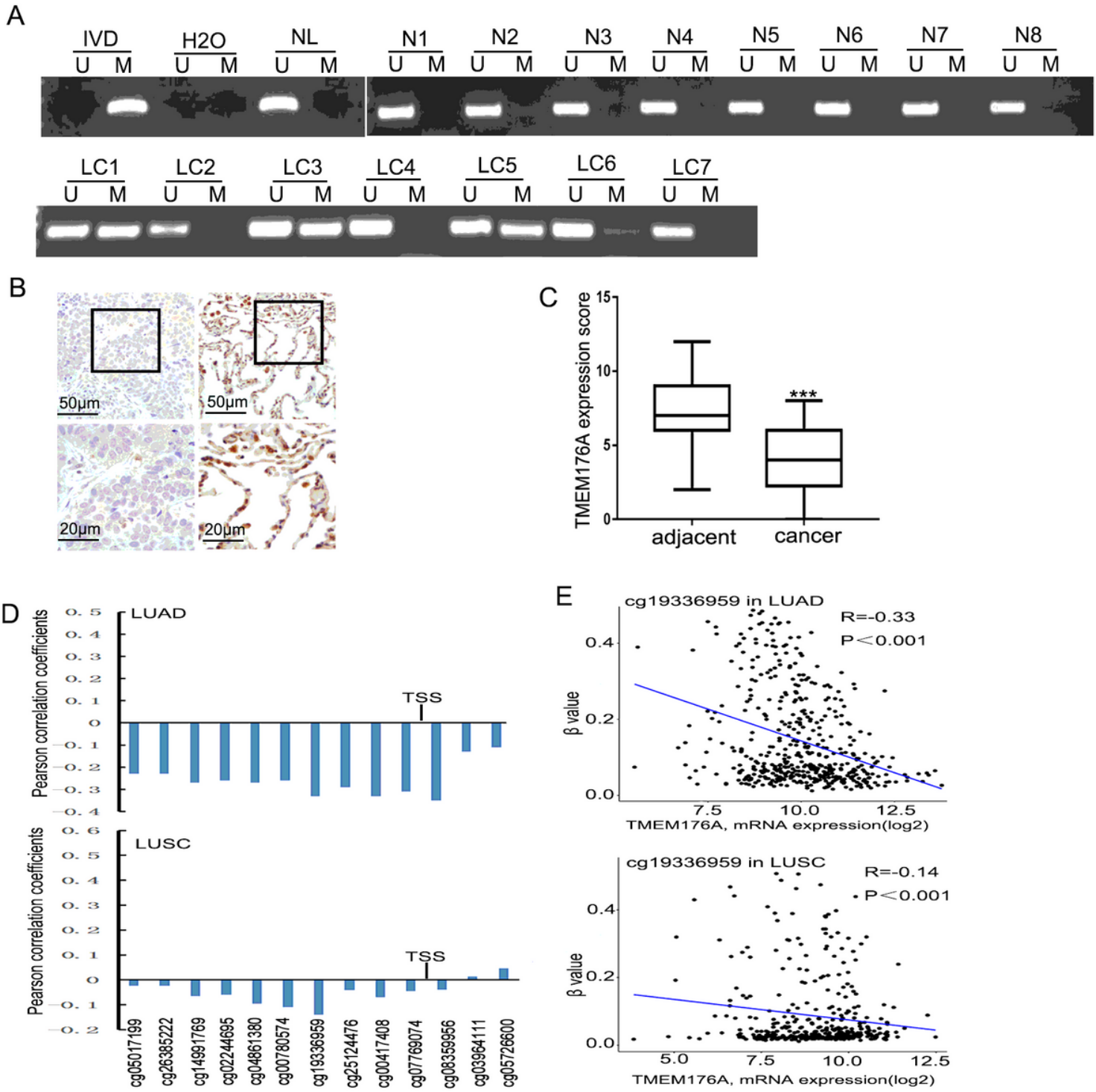

Figure 2

Expression and methylation status of TMEM176A in primary lung cancer A. Representative MSP results of TMEM176A in normal liver tissue samples and primary lung cancer samples. N: normal liver tissue samples; LC: primary lung cancer samples. B. Representative IHC results show TMEM176A expression in lung cancer tissue and adjacent tissue samples (top: ×200; bottom: ×400). C. TMEM176A expression scores are shown as box plots, horizontal lines represent the median score; the bottom and top of the boxes represent the 25th and 75th percentiles, respectively; vertical bars represent the range of data.

Expression of TMEM176A was significantly different between adjacent tissue and lung cancer tissue in 40-matched lung cancer samples. ***P<0.001 D. Pearson correlation coefficient between TMEM176A methylation and expression at each CpG site. LUAD: lung adenocarcinoma, LUSC: lung squamous carcinoma, TSS: transcription start site. E. Scatter plots showing the methylation status of the seventh (cg03964111) CpG sites, which are correlated with loss or reduced TMEM176A expression in 457 cases of lung adenocarcinoma samples and 372 cases of lung squamous carcinoma samples. β-value were considered methylated. ***P < 0.001

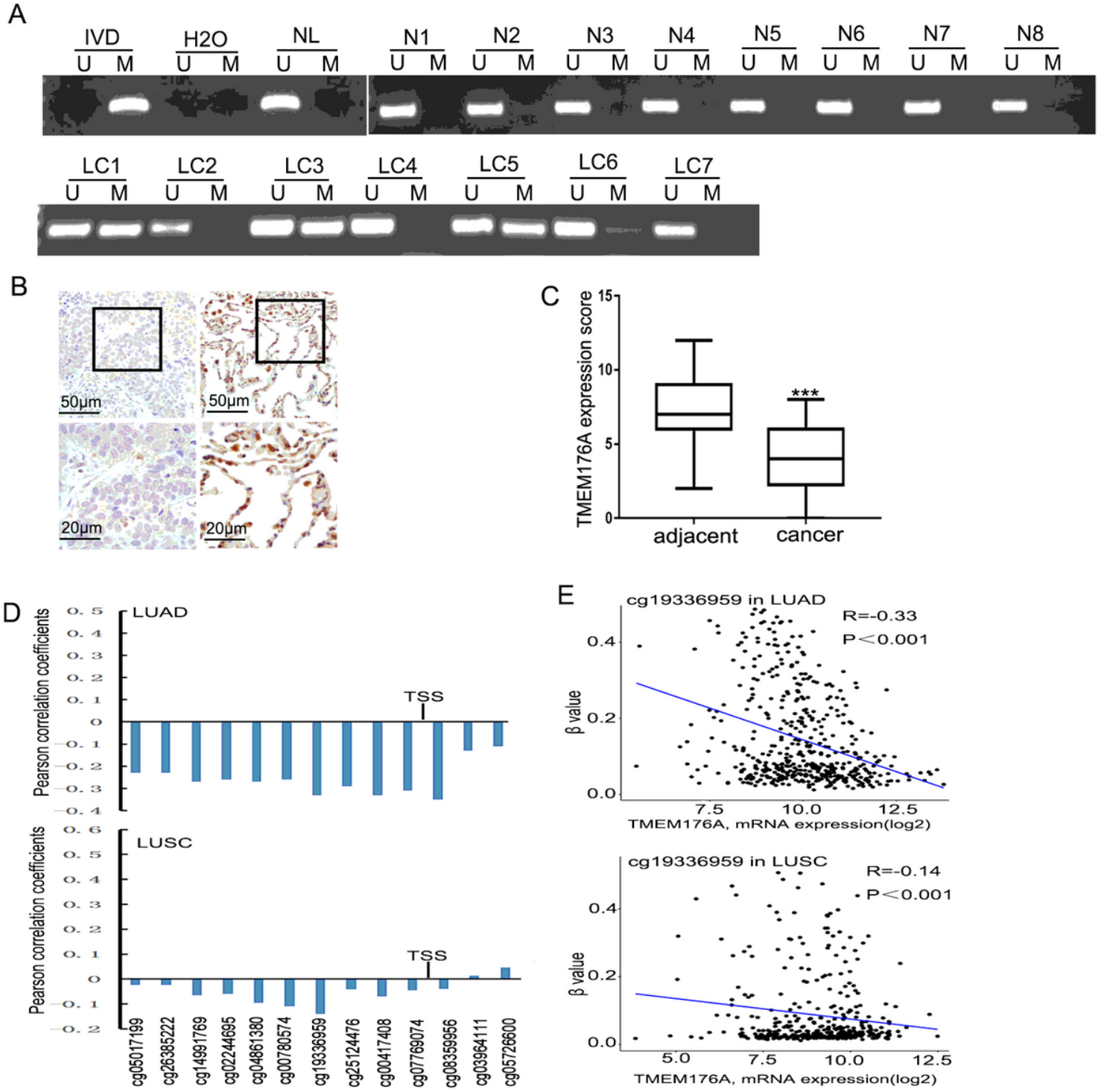

Figure 2

Expression and methylation status of TMEM176A in primary lung cancer A. Representative MSP results of TMEM176A in normal liver tissue samples and primary lung cancer samples. N: normal liver tissue samples; LC: primary lung cancer samples. B. Representative IHC results show TMEM176A expression in lung cancer tissue and adjacent tissue samples (top: ×200; bottom: ×400). C. TMEM176A expression scores are shown as box plots, horizontal lines represent the median score; the bottom and top of the boxes represent the 25th and 75th percentiles, respectively; vertical bars represent the range of data. Expression of TMEM176A was significantly different between adjacent tissue and lung cancer tissue in 40-matched lung cancer samples. ***P<0.001 D. Pearson correlation coefficient between TMEM176A methylation and expression at each CpG site. LUAD: lung adenocarcinoma, LUSC: lung squamous carcinoma, TSS: transcription start site. E. Scatter plots showing the methylation status of the seventh (cg03964111) CpG sites, which are correlated with loss or reduced TMEM176A expression in 457 cases of lung adenocarcinoma samples and 372 cases of lung squamous carcinoma samples. β-value were considered methylated. ***P < 0.001

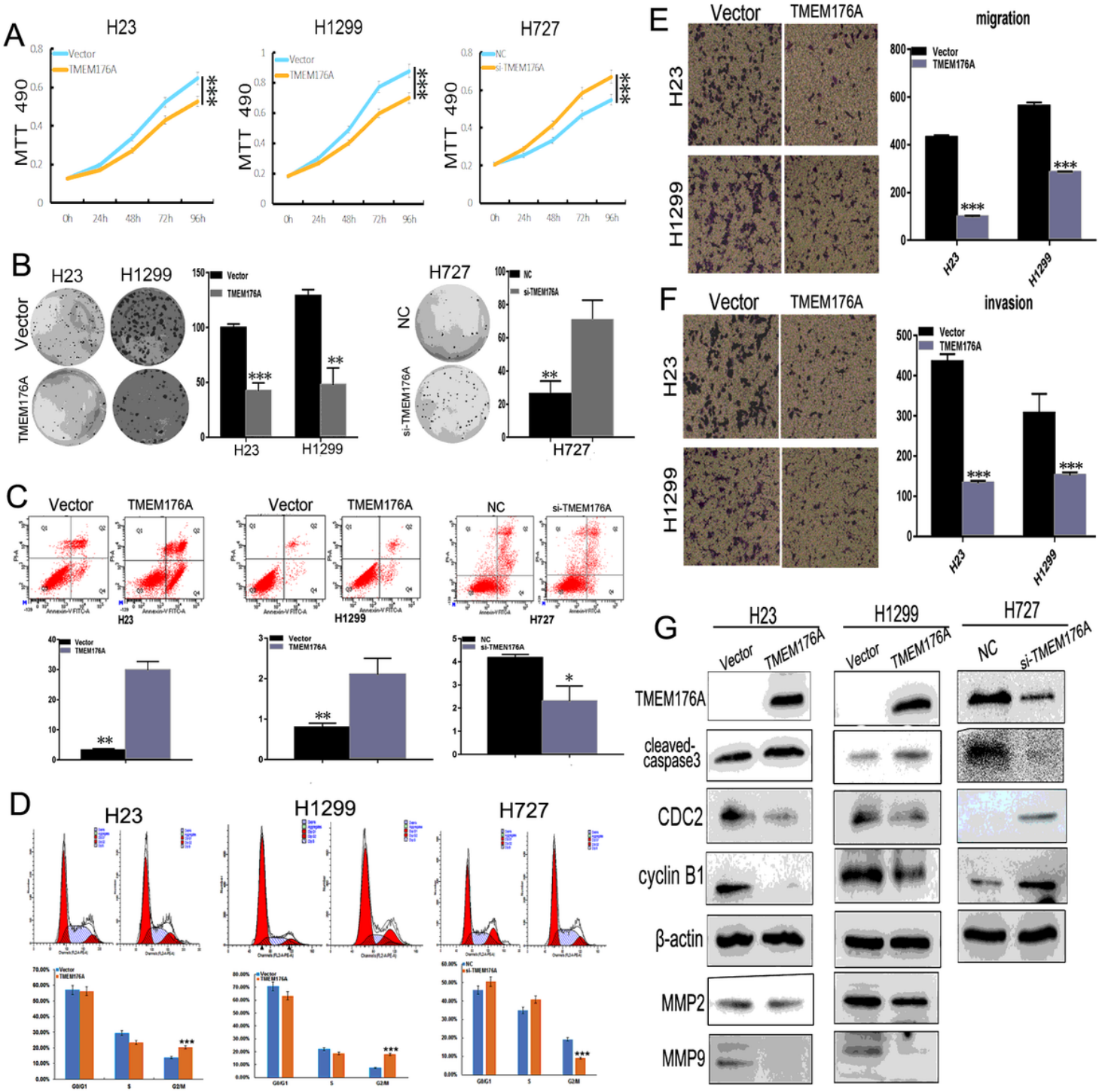

Figure 3

Effect of TMEM176A on lung cancer cell proliferation, apoptosis, invasion and migration. A. Growth curves represent cell viability analyzed by the MTT assay in TMEM176A re-expressed and unexpressed H23 and H1299 cells, as well as in H727 before and after knockdown of TMEM176A. Each experiment was repeated in triplicate. ***P<0.001 B. Colony formation results show that colony numbers were reduced by re-expression of TMEM176A in H23 and H1299 cells, while they were increased by knockdown of TMEM176A in H727 cells. Each experiment was repeated in triplicate. Average number of tumor clones

is represented by bar diagram. **P<0.01, ***P<0.001. C. Flow cytometry results show induction of apoptosis by re-expression of TMEM176A in H23 and H1299 cells, while reduction of apoptosis was found after knockdown of TMEM176A in H727 cells. *P < 0.05,**P<0.01 D. Cell phase distribution in TMEM176A unexpressed and re-expressed H23 and H1299 cells, as well as cell phase distribution before and after knockdown of TMEM176A in H727 cells. Each experiment was repeated three times. ***P < 0.001 E. The migration assays show migration cells before and after restoration of TMEM176A expression in H23 and H1299 cells. ***P<0.001 F. The invasion assays show invasive cells before and after restoration of TMEM176A expression in H23 and H1299. ***P<0.001 G. Western blots show the effects of TMEM176A on the levels of cleaved caspase-3、CDC2、cyclin B1, MMP2 and MMP9 expression in H23, H1299 and H727 cells. Vector: control vector, TMEM176A: TMEM176A expressing vector, β-actin: internal control. NC: siRNA negative control; siTMEM176A: siRNA for TMEM176A

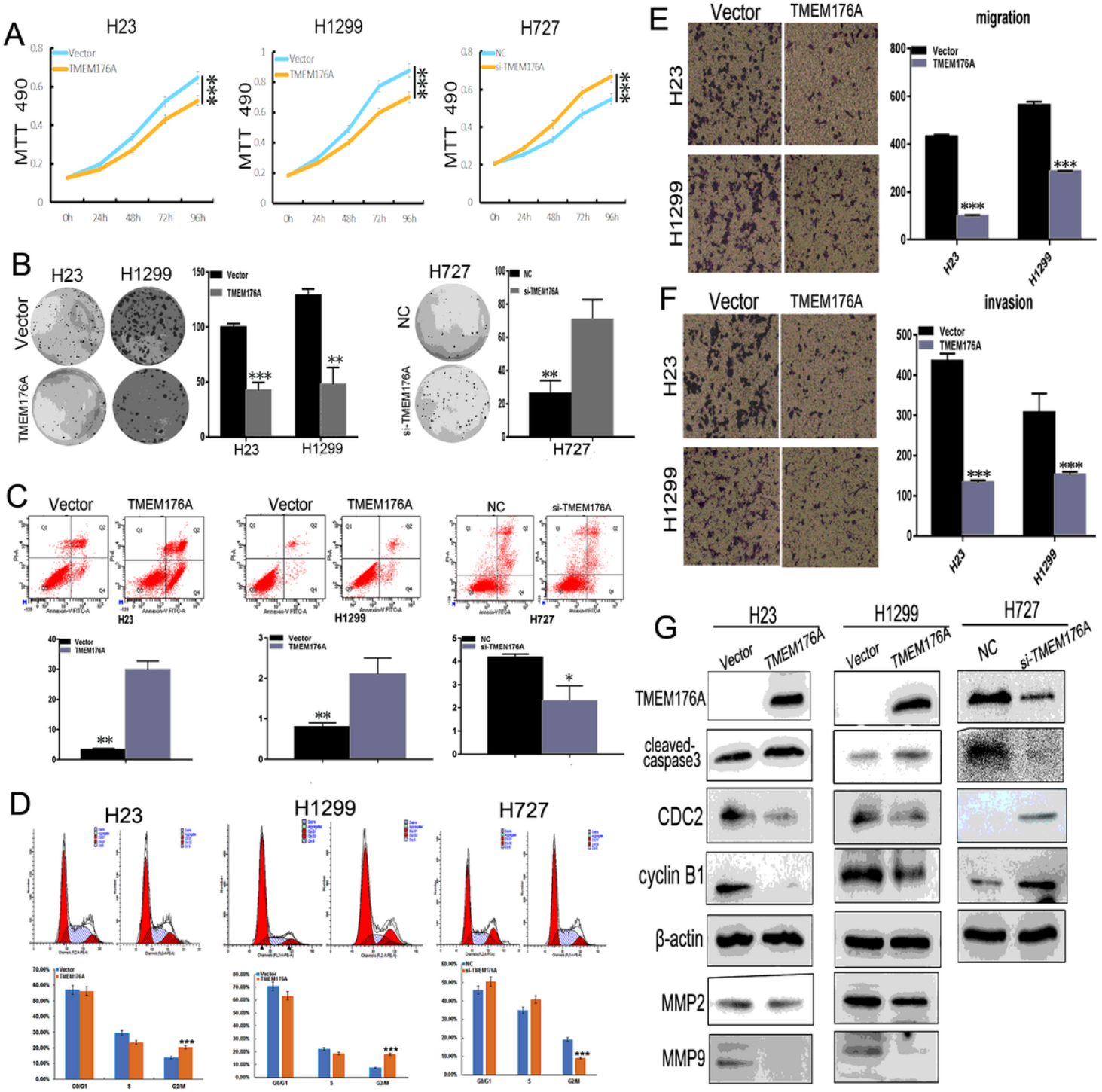

Figure 3

Effect of TMEM176A on lung cancer cell proliferation, apoptosis, invasion and migration. A. Growth curves represent cell viability analyzed by the MTT assay in TMEM176A re-expressed and unexpressed H23 and H1299 cells, as well as in H727 before and after knockdown of TMEM176A. Each experiment was repeated in triplicate. ***P<0.001 B. Colony formation results show that colony numbers were reduced by re-expression of TMEM176A in H23 and H1299 cells, while they were increased by knockdown of TMEM176A in H727 cells. Each experiment was repeated in triplicate. Average number of tumor clones

is represented by bar diagram. **P<0.01, ***P<0.001. C. Flow cytometry results show induction of apoptosis by re-expression of TMEM176A in H23 and H1299 cells, while reduction of apoptosis was found after knockdown of TMEM176A in H727 cells. *P < 0.05,**P<0.01 D. Cell phase distribution in TMEM176A unexpressed and re-expressed H23 and H1299 cells, as well as cell phase distribution before and after knockdown of TMEM176A in H727 cells. Each experiment was repeated three times. ***P < 0.001 E. The migration assays show migration cells before and after restoration of TMEM176A expression in H23 and H1299 cells. ***P<0.001 F. The invasion assays show invasive cells before and after restoration of TMEM176A expression in H23 and H1299. ***P<0.001 G. Western blots show the effects of TMEM176A on the levels of cleaved caspase-3、CDC2、cyclin B1, MMP2 and MMP9 expression in H23, H1299 and H727 cells. Vector: control vector, TMEM176A: TMEM176A expressing vector, β-actin: internal control. NC: siRNA negative control; siTMEM176A: siRNA for TMEM176A

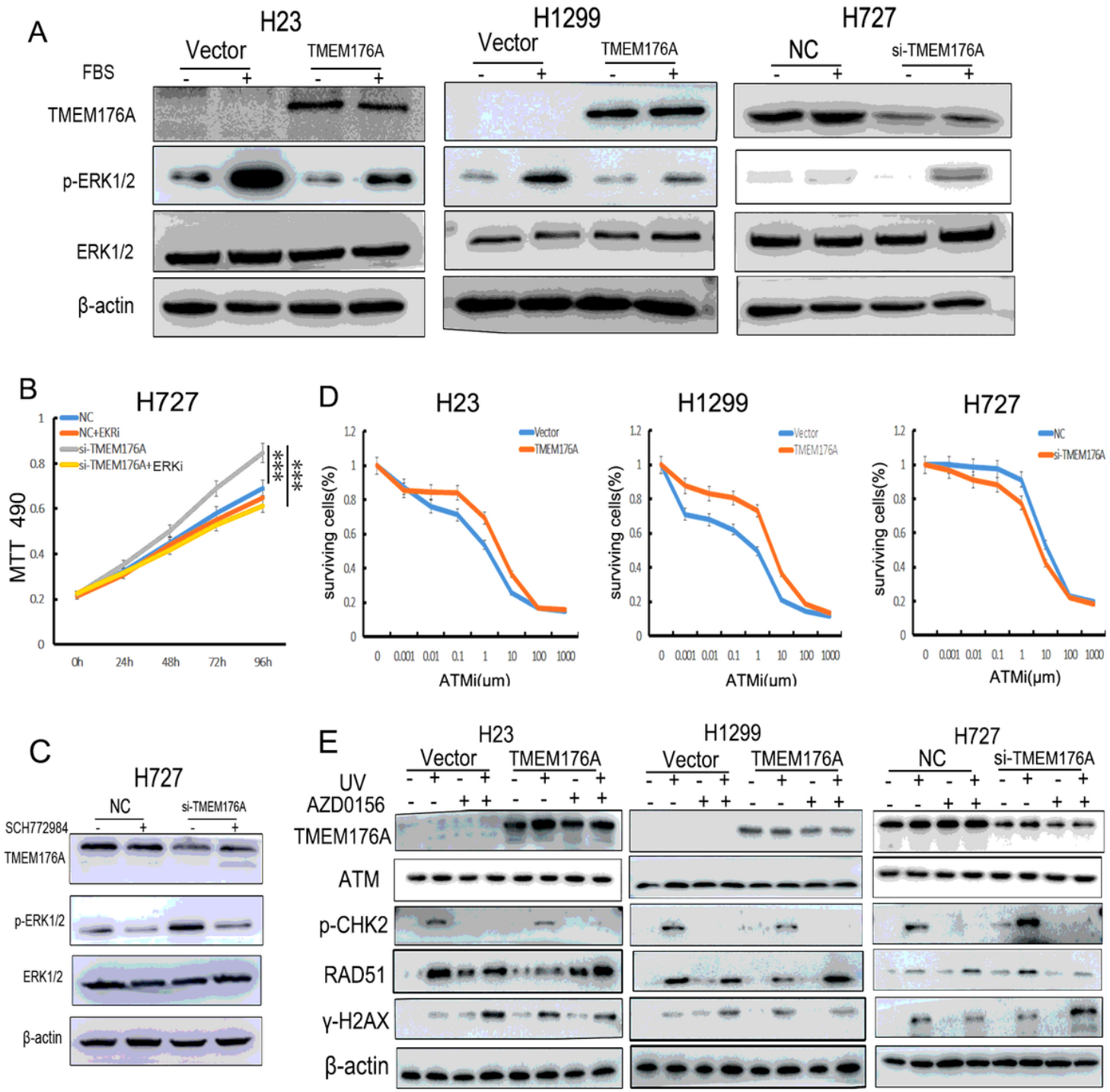

Figure 4

TMEM176A inhibits the ERK signaling pathway, and loss expression of TMEM176A cells are sensitivity to AZD0156. A. Western blots show the levels of TMEM176A, ERK1/2 and p-ERK1/2 in H23, H1299 and H727 cells. β-actin: internal control. -: no serum stimulation. +: serum stimulation B. Growth curves represent cell viability evaluated by MTT assay in the control group, control plus SCH772984 treatment, siTMEM176A group, and siTMEM176A plus SCH772984 treatment group in H727 cell. siTMEM176A: siRNA knockdown of TMEM176A. ***P<0.001 C. The expression levels of TMEM176A, ERK1/2 and p-

ERK1/2 were detected by Western blot. SCH772984: p-ERK1/2 inhibitor; (-): absence of SCH772984; (+): presence of SCH772984. D. Cell viability determined by MTT assays following exposure to AZD0156. E. The expression levels of TMEM176A, γ-H2AX and RAD51 were detected by Western blot. AZD0156: ATM inhibitor(-): absence of AZD0156 or UV; (+): presence of AZD0156 or UV.

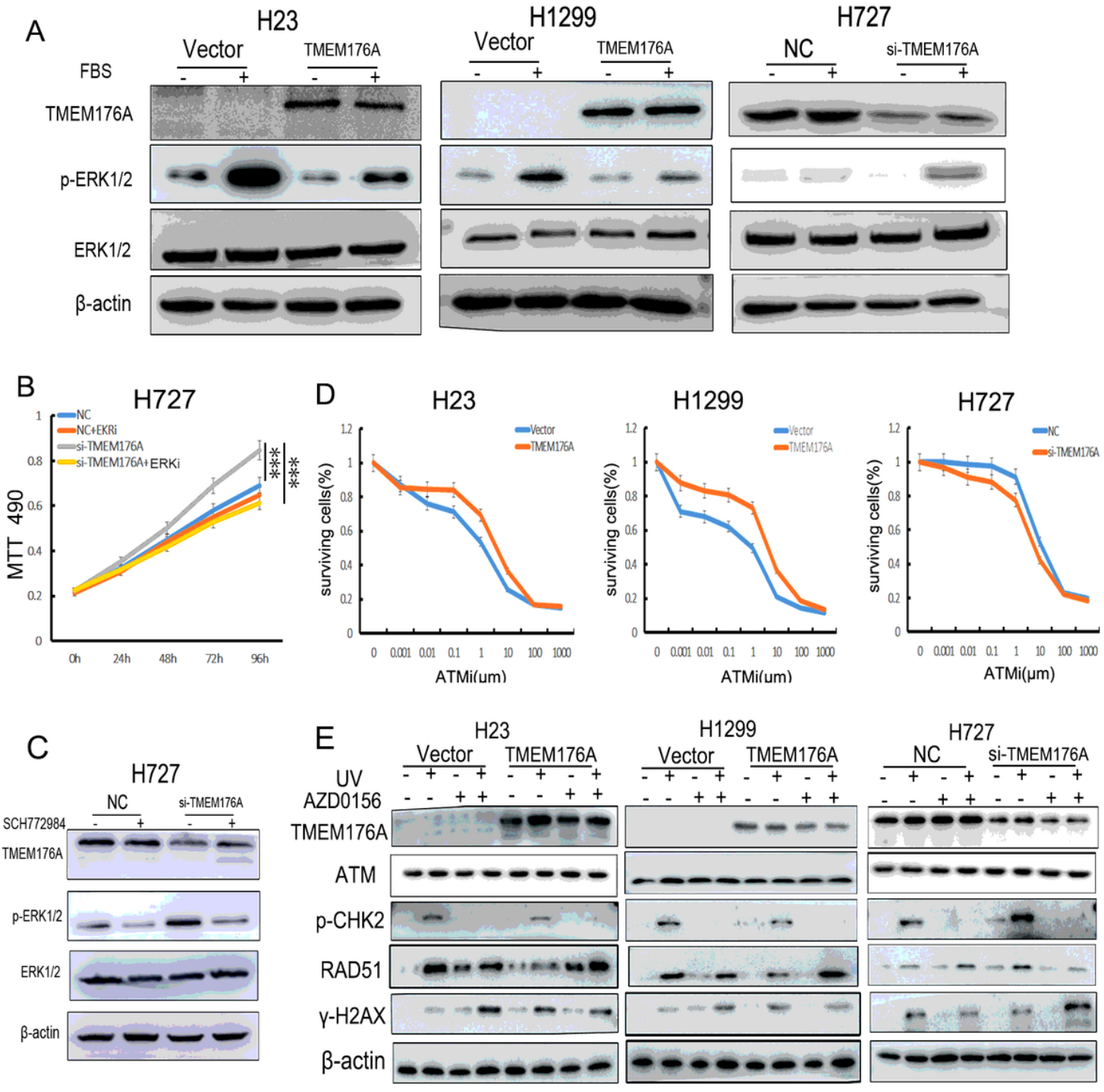

Figure 4

TMEM176A inhibits the ERK signaling pathway, and loss expression of TMEM176A cells are sensitivity to AZD0156. A. Western blots show the levels of TMEM176A, ERK1/2 and p-ERK1/2 in H23, H1299 and

H727 cells. β-actin: internal control. -: no serum stimulation. +: serum stimulation B. Growth curves represent cell viability evaluated by MTT assay in the control group, control plus SCH772984 treatment, siTMEM176A group, and siTMEM176A plus SCH772984 treatment group in H727 cell. siTMEM176A: siRNA knockdown of TMEM176A. ***P<0.001 C. The expression levels of TMEM176A, ERK1/2 and p-ERK1/2 were detected by Western blot. SCH772984: p-ERK1/2 inhibitor; (-): absence of SCH772984; (+): presence of SCH772984. D. Cell viability determined by MTT assays following exposure to AZD0156. E. The expression levels of TMEM176A, γ-H2AX and RAD51 were detected by Western blot. AZD0156: ATM inhibitor(-): absence of AZD0156 or UV; (+): presence of AZD0156 or UV.

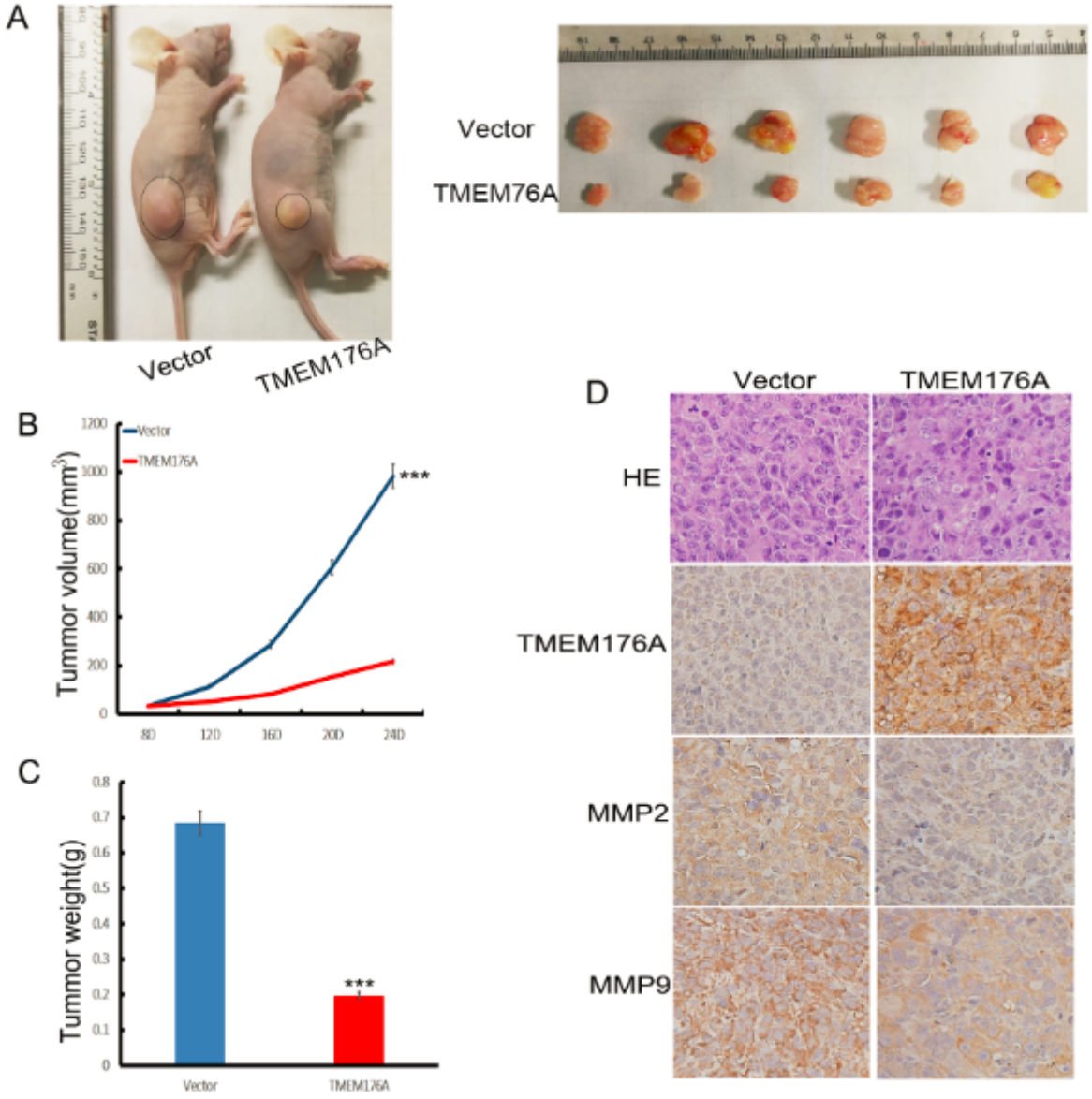

Figure 5

TMEM176A suppresses human lung cancer cell xenograft growth in mice A. Representative tumors from TMEM176A un-expressed and TMEM176A re-expressed H1299 cell xenografts. B. Tumor growth curves of TMEM176A un-expressed and TMEM176A re-expressed H1299 cells. ***P<0.001. C. Tumor weights in nude mice at the 24th day after inoculation of un-expressed and TMEM176A re-expressed H1299 cells.

Bars: mean of 6 mice. ***P<0.001. D. Images of hematoxylin and eosin staining show tumors from TMEM176A un-expressed and TMEM176A re-expressed H1299 xenograft mice. IHC staining reveals the expression levels of TMEM176A, MMP2, MMP9 and p-ERK1/2 in TMEM176A un-expressed and TMEM176A re-expressed H1299 cell xenografts.

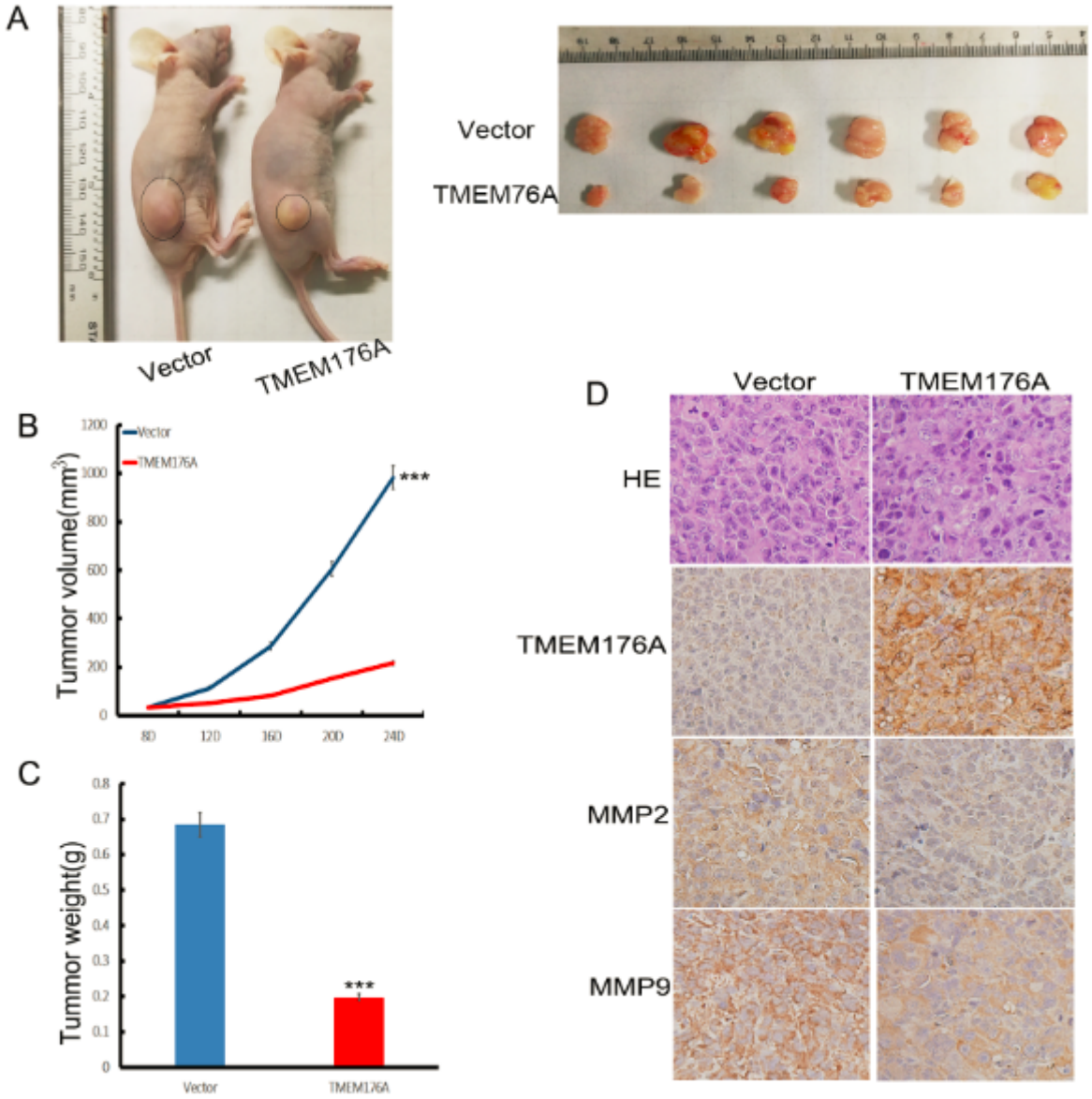

Figure 5

TMEM176A suppresses human lung cancer cell xenograft growth in mice A. Representative tumors from TMEM176A un-expressed and TMEM176A re-expressed H1299 cell xenografts. B. Tumor growth curves of TMEM176A un-expressed and TMEM176A re-expressed H1299 cells. ***P<0.001. C. Tumor weights in nude mice at the 24th day after inoculation of un-expressed and TMEM176A re-expressed H1299 cells. Bars: mean of 6 mice. ***P<0.001. D. Images of hematoxylin and eosin staining show tumors from TMEM176A un-expressed and TMEM176A re-expressed H1299 xenograft mice. IHC staining reveals the expression levels of TMEM176A, MMP2, MMP9 and p-ERK1/2 in TMEM176A un-expressed and TMEM176A re-expressed H1299 cell xenografts.

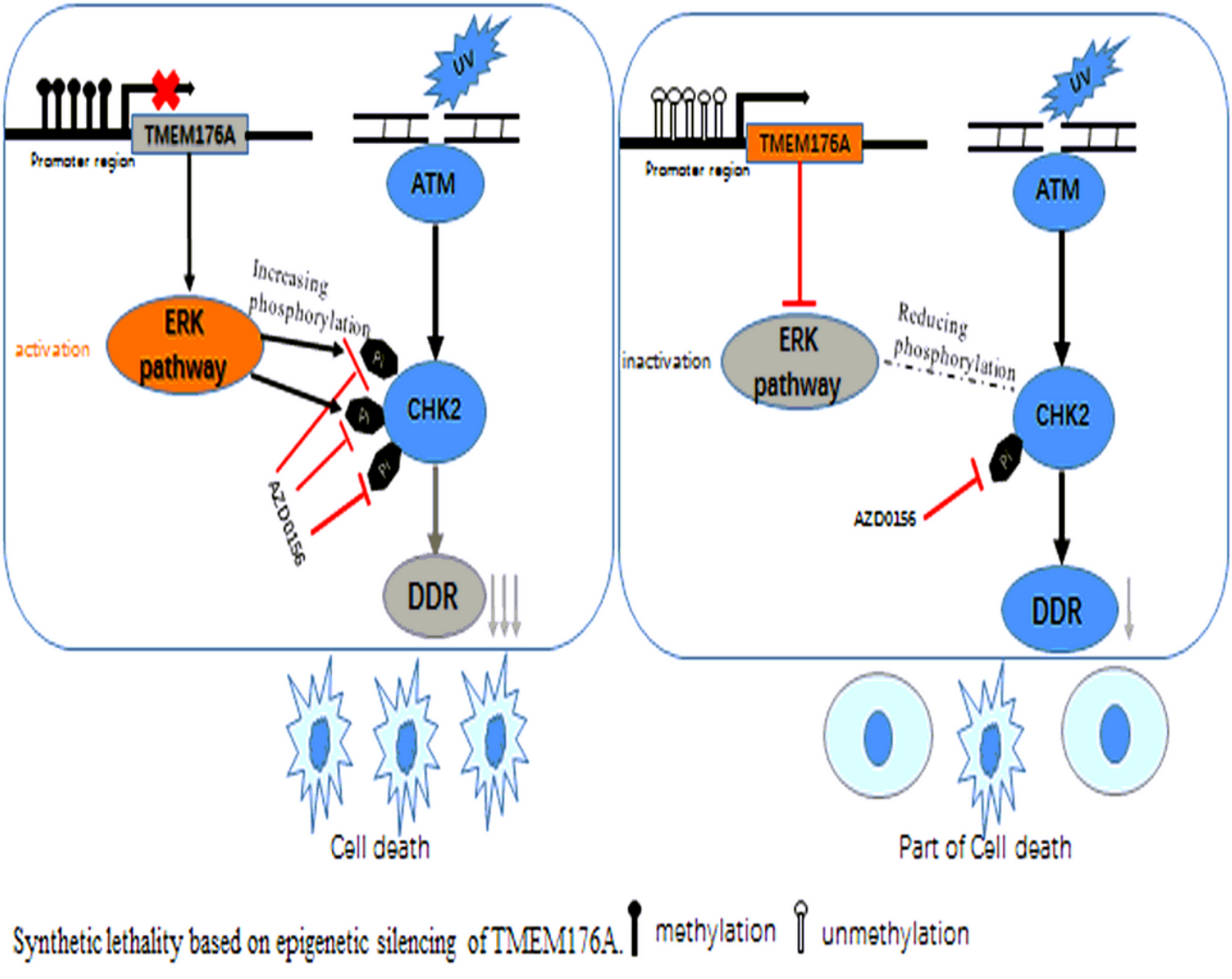

Figure 6

A working model of Synthetic lethality for ATM inhibitor and epigenetic silencing TMEM176A in lung cancer cells

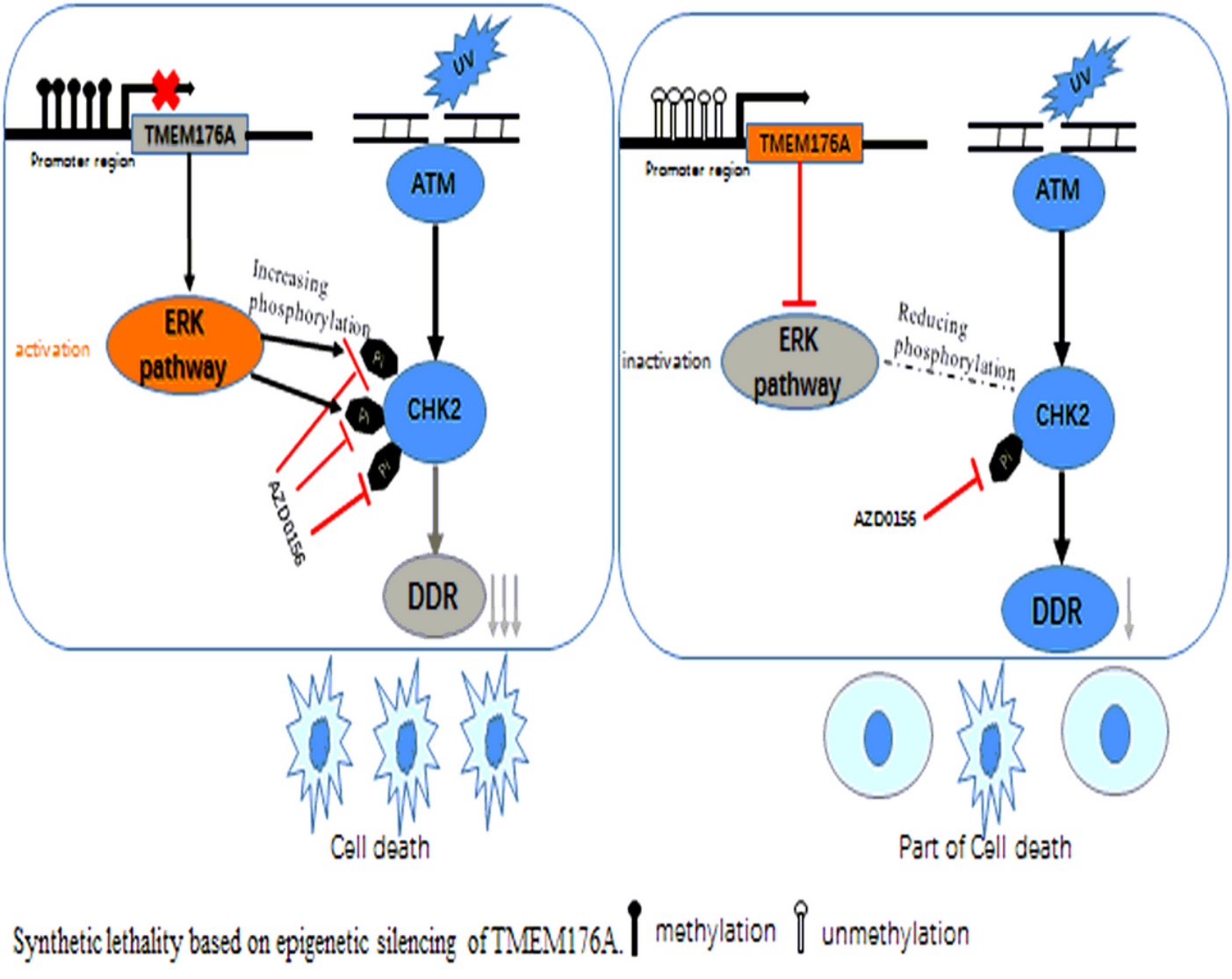

Figure 6

A working model of Synthetic lethality for ATM inhibitor and epigenetic silencing TMEM176A in lung cancer cells